EFFECTS OF THE BRAIN DERIVED NEUROTROPHIC FACTOR VAL66MET POLYMORPHISM ON THE STRUCTURAL AND FUNCTIONAL ARCHITECTURE OF THE HUMAN BRAIN

VICENTE ALBA SUAREZ

A THESIS SUBMITTED TO

THE FACULTY OF GRADUATE STUDIES

IN PARTIAL FULFILLMENT OF THE REQUIREMENTS FOR THE DEGREE OF

MASTER OF ARTS

GRADUATE PROGRAM IN PSYCHOLOGY

YORK UNIVERSITY

TORONTO, ONTARIO

AUGUST 2022

Abstract

Brain Derived Neurotrophic Factor (BDNF) is an important neurotrophin enabling synaptogenesis at the dendrites of neurons. Several studies have implicated the Val66Met single nucleotide polymorphism of the BDNF gene as a factor affecting cortical thickness and resting-state functional connectivity (RSFC) of the human brain. In this thesis, I investigated the effects of Val66Met on cortical thickness and RSFC among individual cortical regions and at the level of large-scale functional networks in all genotype groups (Val/Val, Val/Met, Met/Met, and Met carriers). Cutting-edge techniques were used to individually localize anatomical and functional brain regions in a large sample of healthy young adults from the Human Connectome Project. A comprehensive series of analyses revealed no significant group differences in cortical thickness or RSFC across the brain. These results suggest that, contrary to previous reports, the Met allele does not confer differences in structural or functional integrity of the healthy young adult brain.

Acknowledgments

I would like to express my deepest appreciation to my supervisor, Dr. Dale Stevens, and my thesis committee, Dr. Nathan Spreng and Dr. Georg Zoidl, for their continuous support and guiding my research to new and interesting directions. I am very grateful to the Vision: Science to Application (VISTA) program for awarding me the VISTA Training Scholarship that helped fund my Master's degree and the research presented in this thesis. I could not have undertaken this journey without the help of my colleagues in the Cognition and Aging Neuroscience lab. Words cannot express my gratitude to Katherine Newman, who guided me every step of the way and without whom this study would not have been possible. I would like to extend my sincere thanks to Jared Granger and Michelle Clevett for their assistance in editing, and to Stephan Bonfield for his statistical expertise. I am grateful to all my friends and family, especially my parents, who supported me over this two-year journey and have helped me grow and mature as a scientist and a person. Data were provided by the Human Connectome Project, WU-Minn Consortium (Principal Investigators: David Van Essen and Kamil Ugurbil; 1U54MH091657) funded by the 16 NIH Institutes and Centers that support the NIH Blueprint for Neuroscience Research; and by the McDonnell Center for Systems Neuroscience at Washington University.

Table of Contents

List of Tables

List of Figures

Introduction

Genetic variance can influence the typical functioning of bodily processes, organs, and systems (Carmelli et al., 1998; Jackson et al., 2018; Smit et al., 2012). This has been observed for genes acting on the human brain, including those involved in the formation of synaptic connections between neurons (Pezawas et al., 2004; Ridding & Ziemann, 2010). One of the most important genes in the early development, maintenance, and plasticity of neural pathways is brain derived neurotrophic factor (BDNF), which codes for a protein responsible for synaptogenesis at dendrites (Levine et al., 1998; Patterson et al., 1996). The Val66Met single nucleotide polymorphism (SNP) of the BDNF gene has been studied extensively across various disciplines of neuroscience (Bathina & Das, 2015; Cheeran et al., 2008; Chen et al., 2006; Hall et al., 2003; Pezawas et al., 2004), but the influence this SNP has on large-scale functional brain networks--measured using resting-state functional connectivity (RSFC) analyses of functional magnetic resonance imaging (fMRI) data--has been largely unexplored. The few studies investigating this relationship are limited in sample size and scope, and findings have been inconsistent (Jang et al., 2012; Thomason et al., 2009; C. Wang et al., 2014). The Met allele is known to have a varied distribution across different ethnic groups (Petryshen et al., 2010) and affect the severity and prognosis of various diseases (Duman & Monteggia, 2006; Lim et al., 2016). Considering these findings, this SNP could be impacting the reliability of fMRI studies. Therefore, an analysis of the impact of Val66Met in a larger sample of participants would elucidate whether this genetic difference significantly and reliably affects brain structure and functional integrity within and between brain networks. The proposed research aims to fill this knowledge gap by using the Human Connectome Project (HCP), a large, open-source neuroimaging dataset that includes genetic, behavioural, and lifestyle data in addition to MRI

data from a variety of neuroimaging protocols (Van Essen et al., 2013). With over 1000 participants, the HCP provides a comparatively large sample of neuroimaging and genetic data that can improve our fundamental understanding of the relationship between the BDNF neurotrophin, RSFC, and cortical thickness (CT).

Brain Derived Neurotrophic Factor: a Critical Brain Protein

BDNF is a mammalian protein encoded by the BDNF gene found on human autosomal chromosome 11 and belongs to the neurotrophin family of proteins. BDNF protein was first isolated from pigs (Barde et al., 1982), and has since been studied in rats, mice, and humans (Johnson et al., 1986; Patterson et al., 1996; Rosenfeld et al., 1995). As a neurotrophin, it is instrumental in the synthesis and maintenance of neuron cell bodies, dendrites, and neural pathways (Robinson et al., 1999). As such, BDNF is often associated with neuroplasticity, including the creation and modification of synapses between neurons due to damage and/or learning. The BDNF protein is primarily produced in neuron cell bodies of the cerebral cortex and hippocampus, primarily concentrating at the synaptic bouton (Levine et al., 1998; Patterson et al., 1996). BDNF mediates the creation of new synaptic connections between axon terminals and dendrites by amplifying N-methyl-D-aspartate (NMDA) receptor-mediated currents at the postsynaptic cell (Levine et al., 1998; Xu et al., 2000). BDNF achieves this by binding to extracellular Tropomyosin receptor kinase B (TrkB) receptors found at the cell surface and engaging key signalling pathways to cell survival and neurite formation (Brunet et al., 1999; Klein et al., 1991; Xing et al., 1996). In gene knockout studies performed on mice, the absence of BDNF protein led to noticeably reduced dendritic outgrowths from neurons (Bekinschtein et al., 2008).

An SNP occurs when there is a change in the nucleotide base at a specific locus in the DNA sequence, potentially leading to amino acid coding differences that impact protein structure and function. One of the most well-studied SNPs for BDNF–Val66Met–is the result of a guanine to adenine nucleotide change at position 66 on the pro-peptide, which leads to a valine (Val) amino acid being replaced by methionine (Met) and ultimately its composition (See Figure 1). Individuals with two copies of the Val allele are known as Val homozygotes or Val/Val. Those with one copy of the Met allele are known as Met heterozygotes or Val/Met, and individuals with two copies are known as Met homozygotes or Met/Met. Finally, those with either one or two copies of the Met allele are referred to as Met carriers. Met allele frequencies vary between ethnic populations, ranging from virtually absent in Sub-Saharan Africa, to approximately 25% in most European populations, and as high as 70% for the She population in Asia (Petryshen et al., 2010; see Figure 2). Due to this allelic distribution, studies of this SNP often group Val/Met and Met/Met individuals into a "Met carrier" group to increase sample size.

Figure 1

Visual representation of the Val66Met SNP at codon 66 of exon 1 for the human BDNF gene.

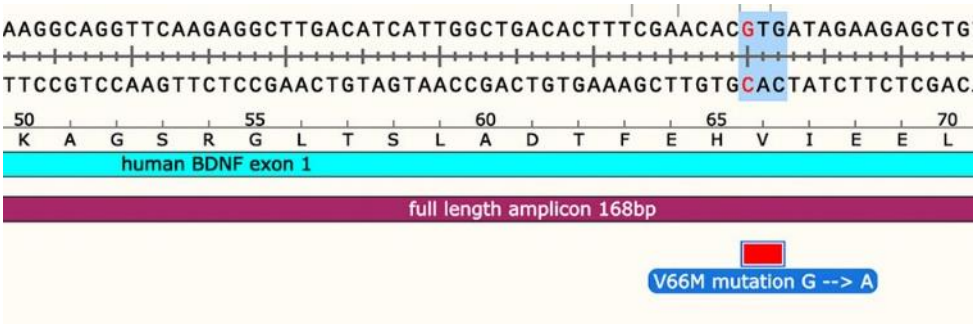

Note. The nucleotide bases of codon 66 are highlighted using a blue rectangle. Letters in red represent the first nucleotide, where the guanine (G) to adenine (A) missense mutation occurs on codon 66, followed by the second and third nucleotide where no changes are observed. Figure provided and adapted courtesy of Dr. Georg Zoidl.

The Val66Met is notable because there has been a great deal of research on the effects of this SNP at various levels of the nervous system. At a cellular level, both heterozygotes and homozygotes for the Met allele produce neurons with shorter and fewer dendritic outgrowths (see Figure 3; Egan et al., 2003). These findings are attributed to a decrease in the activity dependent secretion of BDNF that results from the Met allele. These cellular level changes have been replicated in other human and rodent studies (Chen et al., 2004; Mizui et al., 2015) and are often referenced in higher level studies of behavioural (e.g., Dempster et al., 2005), structural (e.g., Pezawas et al., 2004), and disease differences (e.g., Lim et al., 2021). Despite evidence pointing to these cellular level differences in human and rodent models, studies at the structural and behavioural levels are not as clear-cut on whether and how the Met allele impacts the brain.

Figure 2

Global distribution of the Val66Met SNP of BDNF.

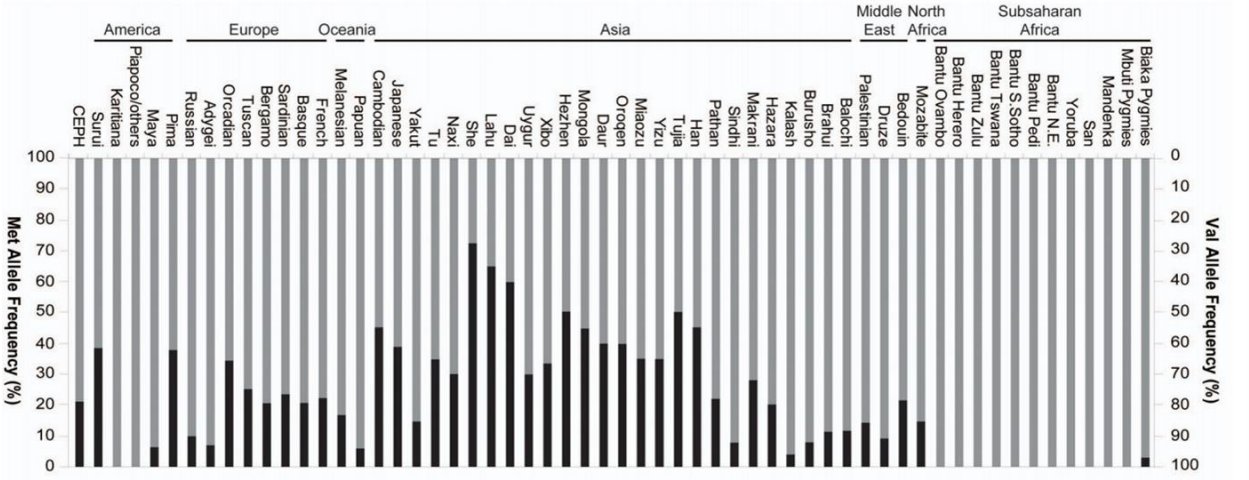

Note. The Met allele frequency can be found on the left y-axis, while Val allele frequency can be found on the right y-axis. These data come from the Centre d'Etude du Polymorphisme Humain (CEPH) dataset, with a total n = 1,157 with data from 57 world populations, and 31 parent-child trios from Ibadan, Nigeria. Reprinted by permission from Springer Nature Customer Service Centre GmbH: Nature, Molecular Psychiatry, Population genetic study of the brain-derived neurotrophic factor (BDNF) gene, Petryshen, T. L., Sabeti, P. C., Aldinger, K. A., Fry, B., Fan, J. B., Schaffner, S. F., Waggoner, S. G., Tahl, A. R., & Sklar, P. Copyright 2009.

For example, studies have observed smaller overall hippocampal volume for Met carriers compared to Val homozygotes (e.g, Bueller et al., 2006; Chepenik et al., 2009; Pezawas et al., 2004; Szeszko et al., 2005). However, other studies have failed to replicate these findings (e.g., Gerritsen et al., 2012; Karnik et al., 2010), and a large meta-analysis by Molendijk and colleagues of hippocampal volume differences identified that while significant differences in volume were observed between healthy Val/Val and Met carriers, all studies were underpowered and the effect sizes observed were close to null (Molendijk et al., 2012). Meanwhile, a small number of studies have investigated CT differences between Val/Val and Met carriers, with one study showing no significant differences between the genotype groups in healthy young adults (C. Wang et al., 2014), another finding that Val/Val had greater thickness in frontal, temporal, and insular regions relative to Met carriers in healthy young adults (X. Yang et al., 2012), and another reporting that occipital and postcentral regions were thicker for Met carrier children relative to Val/Val children (Jasínska et al., 2017).

Other studies have pointed to the Met allele contributing to poorer episodic memory in delayed recall tasks (Dempster et al., 2005; Egan et al., 2003), lower processing speeds in an alphabet-coding task (Miyajima et al., 2008), shorter iconic memory storage (Beste et al., 2011), and decreased performance of verbal learning and memory in healthy individuals (B.-C. Ho et al., 2006). However, a meta-analysis by Mandelman and Grigorenko (2012) that included all previous behavioural studies did not find that healthy Met carriers and Val homozygotes reliably differed on any behavioural measures of general cognitive ability, memory, executive functioning, visual processing, or cognitive fluency.

Figure 3

Comparison between neurons expressing Val66Val BDNF (vBDNF) and Val66Met BDNF (mBDNF), visualized using green fluorescent protein (GFP).

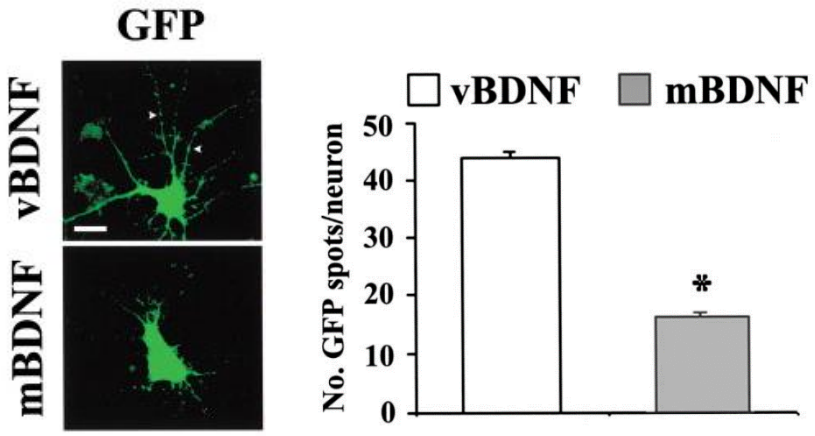

Note. Both SNPs of BDNF were genetically modified to express GFP as a reporter protein. The neuron with vBDNF shows elaborate dendritic outgrowths, while fewer and shorter dendrites are observed in the mBDNF neuron. The graph on the right indicates more GFP expression in vBDNF neurons (n = 50) than in neurons containing the mBDNF (n = 50). Adapted by permission from Elsevier: Cell, The BDNF val66met polymorphism affects activity-dependent secretion of BDNF and human memory and hippocampal function, Egan, M. F., Kojima, M., Callicott, J. H., Goldberg, T. E., Kolachana, B. S., Bertolino, A., Zaitsev, E., Gold, B., Goldman, D., Dean, M., Lu, B., & Weinberger, D. R. Copyright 2003

Potential Differences of Val66Met Genotypes on Intrinsic Functional Networks

The inconclusive evidence from studies of behaviour and structure in groups differing by the Val66Met SNP brings attention to whether this allele could impact interactions of brain networks that are important in the typical functioning of the brain. A limited number of studies have explored the possibility of differences between intrinsic functional brain networks; however, there has been progress in the field relating to the methods used in fMRI data

collection and analysis. To confirm whether differences in intrinsic brain networks exist, further research on the Val66Met SNP using functional neuroimaging is required.

To obtain functional brain images, fMRI captures the blood-oxygen-level-dependent (BOLD) signal, an indirect measure of neural activity. When a group of neurons fire, blood flow is increased to the region to provide oxygen and glucose. fMRI exploits the magnetic differences between oxygenated and deoxygenated hemoglobin to visualize the degree to which brain regions are active at any given time (Ogawa et al., 1990). When a higher BOLD signal is measured in a given region, it reflects greater activity occurring at that location at that point in time, taking into account a known and reliable temporal lag between neuronal firing and the hemodynamic response.

Figure 4

Example of how changes in BOLD signal over time can be used to measure RSFC in the default mode network (blue), dorsal attention network (red), and frontoparietal control network (green).

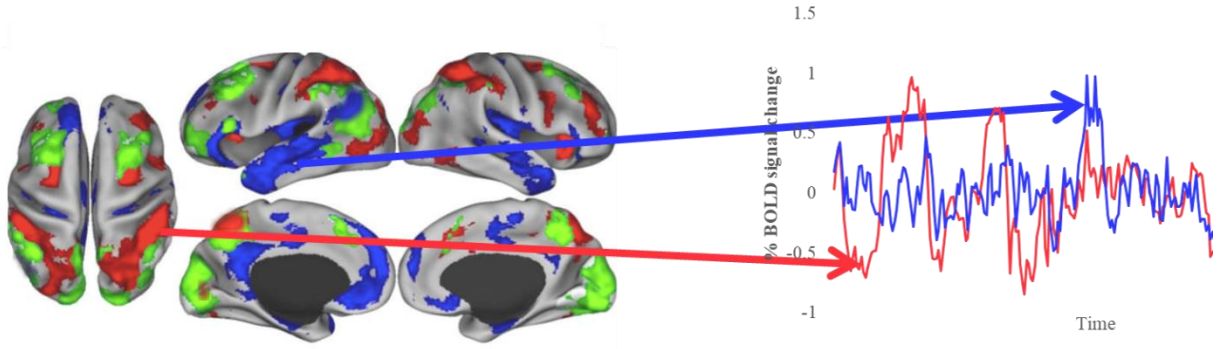

Note. BOLD signal is correlated within like coloured regions, while being distinct among differently coloured regions. The graph on the right indicates little correlation in the BOLD signal between the two regions, indicating low RSFC between these regions. Adapted by permission from Elsevier: NeuroImage, Default network activity, coupled with the frontoparietal control network, supports goal-directed cognition, Spreng, R. N., Stevens, W. D., Chamberlain, J. P., Gilmore, A. W., & Schacter, D. L. Copyright 2010.

Resting-state fMRI (rfMRI) captures spontaneous fluctuations of neural activity over a period of time while the participant is awake and at rest (i.e., typically measured in the absence of any explicit task). RSFC between these regions can be established by measuring spontaneous temporal fluctuations in the BOLD signal among brain regions that are highly temporally correlated (Biswal et al., 1995; Fox et al., 2005). Importantly, spontaneous BOLD signal fluctuations observed in rfMRI can be used to study neural activity in a variety of processes related to cognition, personality, and behaviour (Stevens & Spreng, 2014). This is because the spontaneous BOLD fluctuations that occur at rest follow consistent and replicable spatial patterns that reflect large-scale functional brain networks associated with different functions such as vision, attention, touch and movement, etc. (Schaefer et al., 2018; Yeo et al., 2011). Through rfMRI, researchers can determine RSFC among regions by evaluating pairwise functional connections between regions that covary in their activation over time.

Figure 5

The Yeo 7-network functional brain atlas.

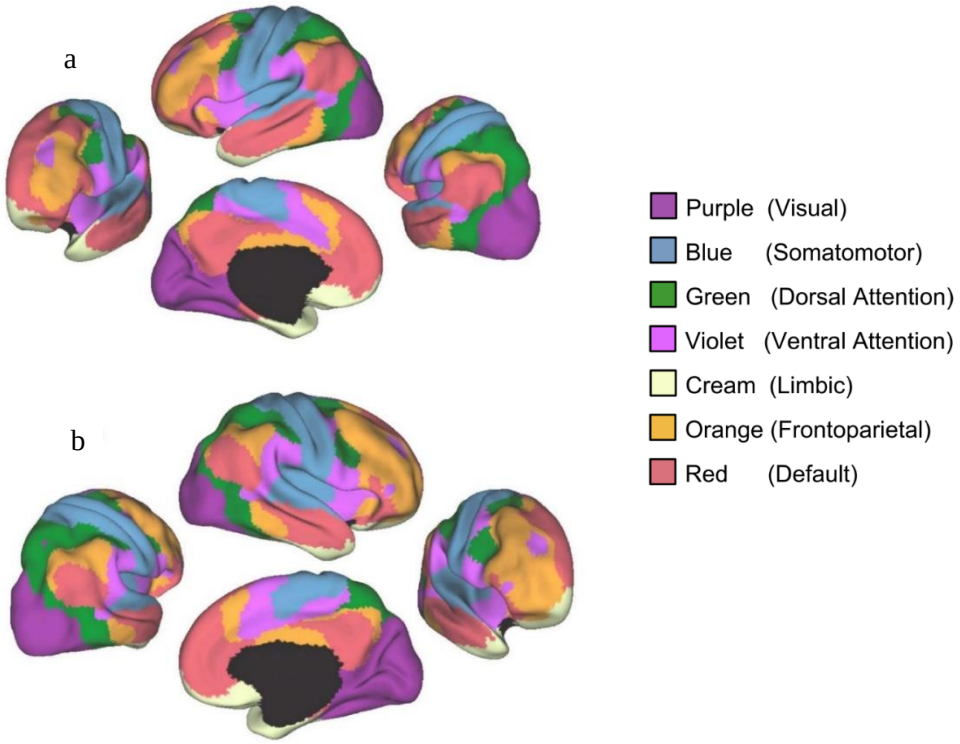

Note. Parcellations for each network were generated from rfMRI collected from 1000 young adults and mapped onto a common structural atlas. Parcellations are shown for both the left (a) and right (b) hemispheres, and for both hemispheres a lateral (top), medial (bottom) anterior (left for (a), right for (b)) and posterior (right for (a), left for (b)) views of the cortical surface is shown. The legend identifies each network as it appears on the cortical surface. Adapted by permission from The American Physiological Society: Journal of Neurophysiology, The organization of the human cerebral cortex estimated by intrinsic functional connectivity, Yeo, B. T., Krienen, F. M., Sepulcre, J., Sabuncu, M. R., Lashkari, D., Hollinshead, M., Roffman, J. L., Smoller, J. W., Zöllei, L., Polimeni, J. R., Fisch, B., Liu, H., & Buckner, R. L. Copyright 2011

Functional brain networks comprise brain regions that coactivate to enable specific sensorimotor, perceptual, and cognitive processes. Regions within these networks need not be topographically adjacent, nor are they necessarily directly connected structurally through axons and synapses. Rather, functional processes will recruit these regions in different combinations,

depending on the task. In typical healthy developing brains of children and adolescents, communication between functional networks becomes increasingly separated while communication within networks becomes increasingly integrated (McIntosh, 2000; Spreng et al., 2013). This concept, termed network differentiation, is a hallmark characteristic of healthy/efficient functional brain network architecture. De-differentiation, such as the changes in network relationships that unfold across the adult lifespan, can impact functional architecture such that within-network connections decline and between-network connections increase (Chan et al., 2014; Setton et al., 2022; Spreng et al., 2016).

Studies have identified various numbers of functionally dissociable networks at various levels of resolution. For instance, Yeo et al. (2011) identified seven unique functional networks with unique brain regions (i.e., region of interest, or ROI) distributed across the brain (see Figure 5). One such network, the default mode network (DMN), is known to activate in relation to internally focused cognitive tasks, including those involving introspection, self-generated thought, and mnemonic representations of ourselves and the world (Andreasen et al., 1995; Andrews-Hanna et al., 2010, 2014; Buckner et al., 2008; Spreng et al., 2010). Conversely, the dorsal attention network (DAN) is linked to externally oriented cognition through top-down control of attention to the external environment (Corbetta & Shulman, 2002). The frontoparietal control network (FPC) acts as a mediator network, selectively modulating and coupling with either the DMN or the DAN depending on the cognitive task. Evidence from Spreng and colleagues (2010, 2013) highlights that while the DMN and DAN are anticorrelated (i.e., the DMN is supressed when the DAN is active, and vice versa), the FPC alternates its connectivity with both and mediates communication between the DMN and DAN.

The Yeo seven-network atlases have since been updated by Schaefer et al. (2018), to establish more refined boundaries and key nodes of each network at multiple parcel resolutions. Atlases like the Schaefer atlas are invaluable assets when performing group comparisons of the brain. By registering each participant's cortical surface to an anatomical template, a group parcellation of the functional networks can be established. This method can allow for analytical comparisons across different groups/conditions, e.g., control vs. experimental group, patient vs. control group, genotype A vs. genotype B, etc. However, atlases assume that the functional parcellations of the group are the same for all participants, and thus do not account for individual differences in the location, size, or shape of parcels between participants (e.g., Glezer & Riesenhuber., 2013). Group results cannot, therefore, be reliably mapped back onto an individual.

Whole brain parcellation methods, such as "group prior individual parcellation" (GPIP), aim to generate a group-based parcellation of the brain, common to all participants at the level of network components, while preserving the finer individual differences in the spatial properties (e.g., size, location, shape) of the nodes of these functional networks (Chong et al., 2017). Therefore, GPIP allows for between-group parcel comparison while creating parcel boundaries specific to each participant, leading to more accurate and consistent functional regions. The result is a more accurate comparison of functional brain networks at both the subject and group-level.

As mentioned earlier, there is evidence to suggest that the Val66Met polymorphism of the BDNF gene can impact RSFC in various brain networks. Studies in both children and adults show reduced RSFC within the DMN (Thomason et al. 2009; Jang et al. 2012), as well as reduced RSFC within the FPC and increased paralimbic RSFC in children (See Figure 6;

Thomason et al. 2009). On the other hand, Wang and colleagues (2014) suggest that Met allele carriers in the Han Chinese population do not have lower RSFC; in fact, these individuals had stronger RSFC between the right anterior insula and dorsolateral prefrontal cortex (DLPFC). While these studies suggest that Val/Val and Met carriers do display differences in both children and healthy young adults, each used seed-based analyses of RSFC based on either literature coordinates or from structural differences. Despite being relatively simple methods to employ, seed-based analyses often do not accurately account for differences between individual subjects because they rely on atlases to localize regions, which may introduce confounding RSFC measures from other networks in group analyses (Cole et al., 2010; Gordon et al., 2015).

Despite methodological limitations, these studies raise important questions about whether the Val66Met polymorphism consistently affects RSFC in brain networks, and if so, in what way. Furthermore, while these effects have been observed in the DMN and FPC, more research is needed to determine how the whole-brain functional connectome is impacted, since differences in RSFC between different genotypes might manifest as behavioural differences or psychiatric and neurodegenerative disorders, such as eating disorders, anxiety, and Alzheimer's disease (Chen et al., 2006; Pezawas et al., 2004; Ribasés et al., 2004).

Figure 6

Comparison of averaged RSFC differences in the DMN, FPC, and paralimbic network between Val homozygotes and Met carriers in children.

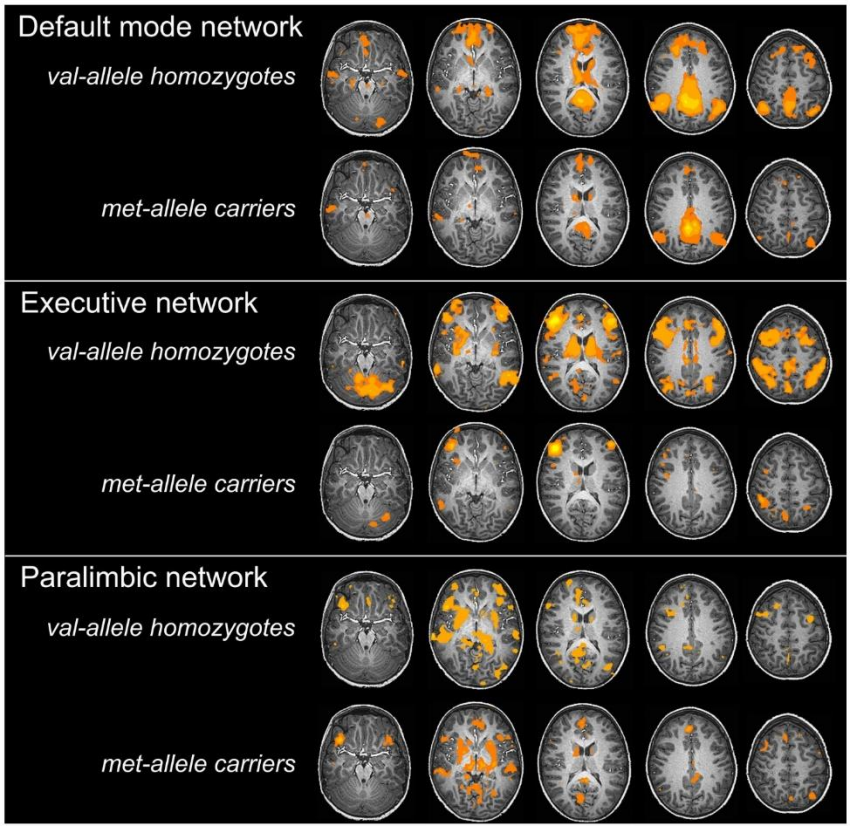

Note. The FPC is labelled as the executive network in this figure. The following seeds were used to capture RSFC: DMN, right PCC: 10, −50, 30; FPC, right DLPFC: 44, 36, 20; Salience Network, right pars orbitalis : 38, 26, −10; MNI coordinates used. Ages of the subjects ranged from 9-16 (mean age ± SD = 12.2 ± 2.1, n = 38, female = 25). Data were collected using rfMRI. Val/Val participants had greater RSFC in the DMN and FPC (but not the paralimbic network) relative to Met carriers, as seen by the higher number of coloured regions and the darker orange shades. Reprinted by permission from Frontiers Research Foundation: Frontiers in Human Neuroscience, BDNF genotype modulates resting functional connectivity in children, Thomason, M. E., Yoo, D. J., Glover, G. H., & Gotlib, I. H. In the public domain. Copyright 2009.

Application of Large Datasets in Neuroimaging Studies and Hypotheses

Findings of impacted RSFC within different brain networks in Met allele carriers point to an interesting and potentially impactful relationship between genotype and brain network connectivity. However, due to the limited sample sizes and the use of methods that do not account for individual differences in functional brain regions, it cannot be concluded with certainty that the differences in RSFC are linked to genotypic variance of BDNF. Larger sample sizes are critical to studies of genetic variability as they provide the necessary statistical power to adequately identify and characterize related differences and are more generalizable to a population level. Due to the high cost of MRI scanning (both monetary and time), studies that involve fMRI are often limited to small sample sizes. For example, the median sample size of neuroimaging studies conducted in 2018 was approximately 24 participants (Szucs & Ioannidis, 2020).

To better quantify and characterize the potential impacts of a genetic polymorphism on functional brain networks at a population level, a large neuroimaging dataset is key. These datasets can contain hundreds to thousands of participants with neuroimaging, genetic, behavioural, demographic, and lifestyle data. Importantly, the extensive amount of data collected in these datasets can allow researchers to exercise a high degree of control for specific combinations of factors. The larger sample sizes in these studies are important in studies of genetic variance for 1) determining how widespread the SNP is, 2) determining whether different ethnic groups have protective factors against the SNP's effects, and 3) eliminating biases that might be found in studies with smaller sample sizes.

The HCP comprises a series of studies that have gathered extensive neuroimaging, genetic, task/behavioural, demographic, and lifestyle data for various groups (both healthy and

diseased) across the lifespan. The HCP dataset has been used extensively as a source for secondary analysis, with the original study having been cited over 2800 times. Their "Young Adult" dataset features approximately 1200 participants ranging from ages 22-35 years old, with demographic information including handedness, drug use, parental history of neurological and psychiatric disease, among many other variables. The volume and detail of the data make the HCP a highly valuable resource to study differences in CT and RSFC between genotypically different groups for Val66Met.

The proposed study will use the HCP Young Adult dataset to perform a whole-brain connectome analysis of RSFC in healthy young adults with different genotypes for the BDNF Val66Met SNP. Potential structural differences in CT between groups will also be investigated to determine whether genotype influences on RSFC are related to differences in brain structure. Based on previous research, including the results of my undergraduate research thesis, I hypothesize that:

1. The Met allele will have a deleterious effect on the functional integrity of resting-state networks, as measured by network differentiation (i.e., high within-network to between-network RSFC ratio). Therefore, functional integrity will decrease in a stepwise manner with more copies of the Met allele, such that the Val/Val group will have typical network differentiation, the Met/Met group will have the least network differentiation, and the Val/Met group will have intermediate network differentiation between that of the Val/Val and Met/Met groups.
2. The Met allele will have a deleterious effect on the structural integrity of the cortex, as measured by CT. Therefore, structural integrity will decrease in a stepwise manner with more copies of the Met allele, such that the Val/Val group will have typical CT, the

Met/Met group will have the least CT, and the Val/Met group will have intermediate CT between that of the Val/Val and Met/Met groups.

Materials and Methods

Data from the HCP Young Adult dataset were used for all analyses in this study. These data were collected by Van Essen et al. (2013) and have been made available for use in secondary analyses. Comparisons of CT between genotype groups for the Val66Met SNP of BDNF were conducted on FreeSurfer CT output data and Val66Met genotype data acquired from the ConnectomeDB database (Marcus et al., 2011). The genetic data/analyses presented in the current thesis are based on the use of study data downloaded from the dbGaP web site, under phs001364.v1.p1 (e.g., https://www.ncbi.nlm.nih.gov/projects/gap/cgi-bin/study.cgi?study_id=phs001364.v1.p1; Mailman et al., 2007). Comparisons of RSFC between genotype groups were performed on RSFC data processed using the GPIP algorithm provided courtesy of Dr. Nathan Spreng.

Participants

Participant data were collected as part of the Human Connectome Project (HCP) 1200 subject release dataset. All participants from the HCP Young Adult dataset were recruited from a population of 22–35-year-old groups of twin and non-twin siblings. None of the participants had any major neurological diseases, psychiatric disorders, or mental health disorders. For a full list of selection criteria, refer to Supplemental Table 1 in Van Essen et al. (2013). Participants were selected such that there were no statistical differences in age or education. Of the total 1029 participants for which both GPIP and genotype data were available, only one individual from any group of siblings was randomly selected for this study to eliminate confounds of genetic overlap

within or between participant groups, resulting in a sub-sample of n = 392 for CT analyses (Val/Val = 257, Val/Met = 121, Met/Met = 14). A subset of this sample was selected for the RSFC analyses based on several exclusion criteria, including drug use (McCulloch et al., 2022; Müller et al., 2021; Sutherland et al., 2012), a breathalyzer test over .05% blood alcohol content (Khalili-Mahani et al., 2012), parental history of psychiatric disorder (Fox & Greicius, 2010; Woodward & Cascio, 2015), handedness (Knecht et al., 2000; Somers et al., 2015), and quality control flags of severe head movement (Friston et al., 1996) (see Figure 7 and Appendix A). A total of 281 right-handed, genetically unrelated participants were selected. Participants were separated into groups according to their BDNF Val66Met polymorphism: (Val/Val n = 187), (Val/Met; n = 80), (Met/Met; n = 14). Additionally, the Val/Met and Met/Met groups were combined to form a Met carrier group for comparisons of all participants with a Met allele; this group was used in every analysis (n = 135 for structural subgroup, n = 94 for functional subgroup).

Figure 7

Breakdown of participants in the Val/Val, Val/Met, and Met/Met groups following application of exclusion criteria to create a functional analysis subset.

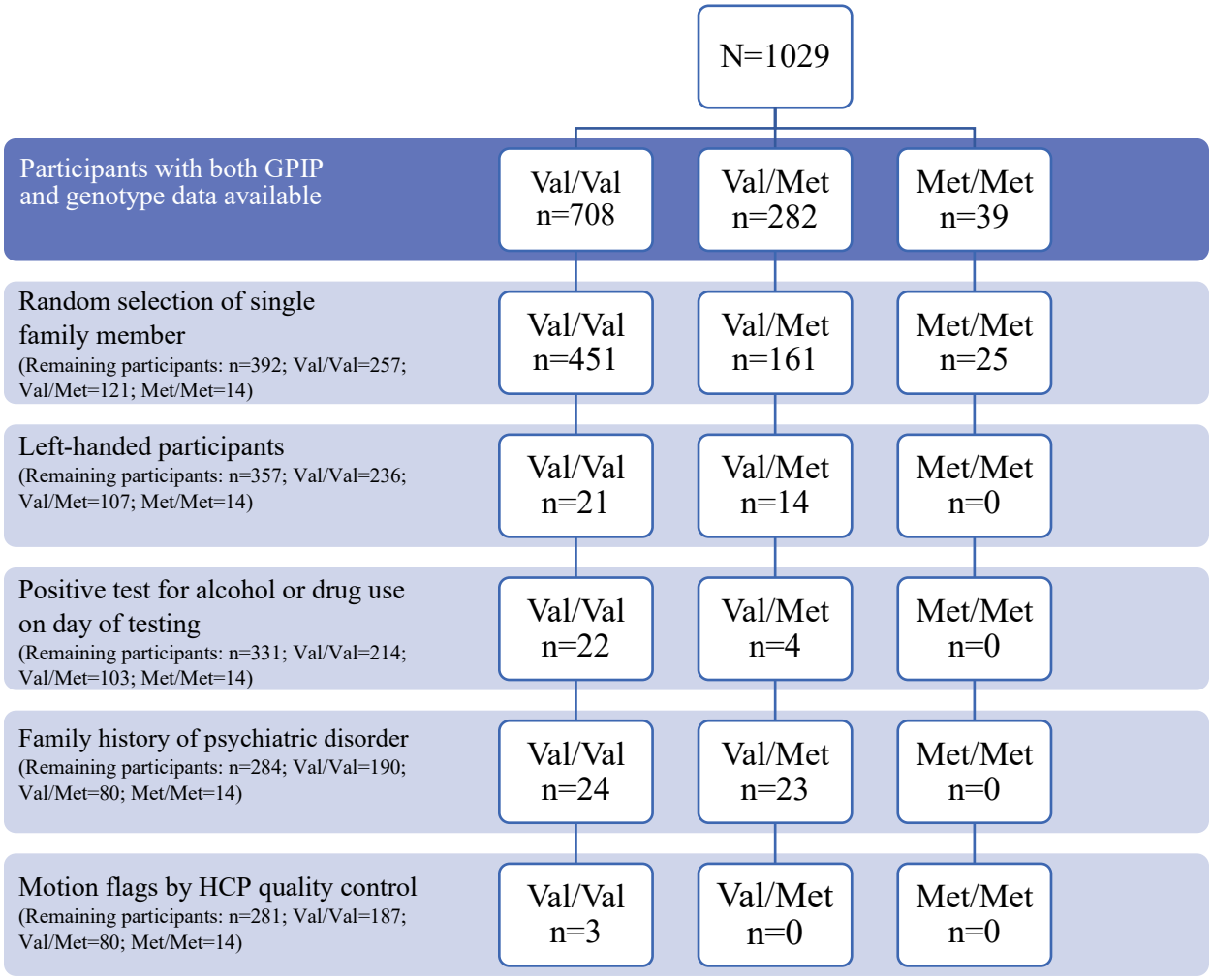

Note. The numbers included in the first row of boxes represent the total number in each genotype group, while the numbers in the following rows of boxes represent how many participants were excluded based on the listed exclusion criteria. From the HCP Young Adult dataset, 1029 had both GPIP parcellations and genetic data available. Of these, participants were randomly selected such that only one member of each family was selected (n=392). Factors with the potential to influence RSFC (e.g., drug use) were used as exclusion criteria, resulting in 281 participants in the functional analysis. Drug tests included THC, opiates, amphetamines, methamphetamines, and oxycontin. Parental history of psychiatric disorder(s) was reported by the participant. Handedness was measured using the Edinburgh Handedness Inventory (Oldfield, 1971). Participants flagged for

motion during one or more rfMRI scans had a significant coil- or movement-related artifact and errors during independent component analysis.

Neuroimaging Acquisition

All HCP participants included in the analyses were scanned on a customized Siemens 3T Connectome Skyra MRI scanner at Washington University in St. Louis (see Table 1 for relevant scan parameters). All MRI data (including structural, functional, and diffusion MRI) for each participant were collected over four 1-hour sessions. Two of the sessions included the collection of rfMRI data, which were acquired in two 15-minute runs per session (four RSFC runs total per participant), during which participants were instructed to keep their eyes open and fixate on a light cross against a dark background. For a full overview of the scanning protocol, refer to the WU-Minn HCP 1200 Subjects Release: Reference Manual and Appendix I.

Table 1

MRI scan parameters for the Human Connectome Project - Young Adult population including structural (T1w) and rs-MRI (Rest).

Type	Description	TR (ms)	TE (ms)	Slices	Flip Angle	FOV (mm)	Matrix	Voxel Size	Acquisition Time (min:sec)
T1w	3D MPRAGE	2400	2.14	256	8 deg	224x224	320x320	0.7 mm isotropic	7:40
Rest	Gradient-echo EPI	720	33.1	72	52 deg	208x180	104x90	2.0 mm isotropic	14:33

Note. Adapted from Glasser et al., 2013 and WU-Minn HCP 1200 Subjects Release: Reference Manual.

Figure 8

Flowchart of methods used in this study.

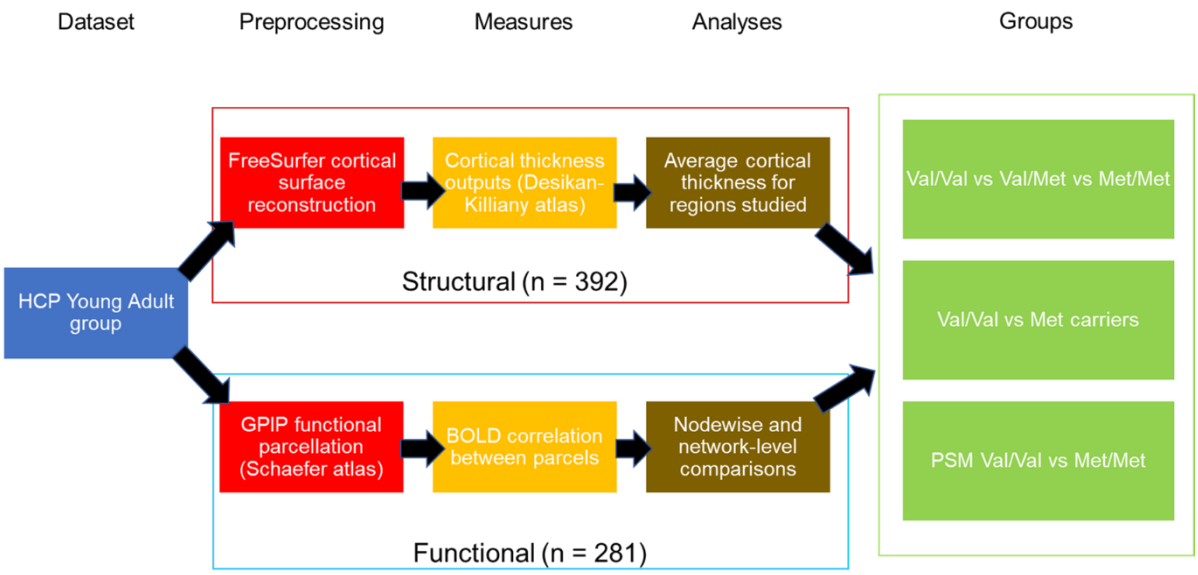

Structural Analysis

A secondary analysis was conducted on the CT values from the HCP FreeSurfer output files provided by the ConnectomeDB database (Marcus et al., 2011). CT was calculated using FreeSurfer, a software package capable of reconstructing the cortical surface using the T1-weighted images from MRI scans (Dale et al., 1999; Fischl & Dale, 2000). These data were preprocessed using the minimal preprocessing pipeline (Glasser et al., 2013). Briefly, three structural pipelines were employed to remove noise and distortions, create cortical maps and segmentations, and align data to a common MNI atlas. A full description of the pre-processing pipeline can be found in Glasser et al. (2013). CT analyses were conducted to compare structural differences between genotype groups. Analyses of CT provide insightful measurements of brain health at the level of the gray matter layer, wherein reductions in CT in different regions may suggest an abnormality afflicting the brain (Querbes et al., 2009).

Preprocessing

Through the minimal preprocessing pipeline described by Glasser et al. (2013), T1-weighted structural brain scans for each participant were segmented and classified into different tissue types (i.e., grey matter, white matter, and cerebrospinal fluid). The left and right hemispheres were then separated while the brainstem and cerebellum were removed. Lastly, FreeSurfer generated a reconstruction of the grey and white matter surfaces.

CT Measures

Alongside the reconstruction of grey and white matter surfaces, FreeSurfer calculates CT as the shortest distance from the newly established pial and white matter surfaces. This process was applied to all participants to acquire a CT measure each of 34 regions of interest (ROIs) in each hemisphere (68 total) corresponding to the Desikan-Killiany atlas, a structural atlas that divides the brain into distinct ROIs in each hemisphere based on gyral separation between regions (Desikan et al., 2006).

ROI Selection

Previous studies have identified differences between Val66Met groups in CT using FreeSurfer for the following bilateral ROIs: inferior parietal cortex (IPC), insula (INS), lingual gyrus (LING) postcentral gyrus (PG), posterior cingulate cortex (PCC), precuneus cortex (PCUN), superior frontal gyrus (SFG), superior temporal gyrus (STG) (Jasínska et al., 2017; C. Wang et al., 2014; X. Yang et al., 2012). Furthermore, these ROIs belong to the DMN and FPC, where differences in RSFC have previously been reported between genotype groups for BDNF Val66Met (Jang et al., 2012; Thomason et al., 2009). Therefore, CT analyses were focused on these ROIs.

Statistics

A one-way analysis of co-variance (ANCOVA) controlling for biological sex was performed to evaluate whether the Val66Met SNP influenced CT at the ROIs listed above. This comparison was performed for all genotype groups (Val/Val, Val/Met, and Met/Met). Any significant results were further investigated with post-hoc analyses. A Mann-Whitney U test was also conducted between the Val/Val and Met carrier groups. The Mann-Whitney U is a non-parametric alternative to Student's t-test that is resistant to violations of variance and normality that may arise due to group size differences (Wilcoxon, 1945).

Functional Analysis

A secondary analysis was conducted on RSFC correlation matrices data provided courtesy of Dr. Nathan Spreng. These data were acquired from the first rFMRI run (15 minutes) collected during the first session. Preprocessing was conducted using the minimal preprocessing pipeline (Glasser et al., 2013). This included the three structural pipelines described earlier, as well as two functional pipelines to remove spatial distortions, perform motion correction, align and register the functional scans to the structural scan, and spatially smooth the data with a 2 mm full width at half maximum Gaussian kernel. Preprocessed data were used as an input for the GPIP algorithm to delineate functional parcels specific to each participant. The normalized BOLD signal timeseries were used to generate RSFC matrices of pairwise ROI correlations for every participant. I then used these matrices to quantify group differences in RSFC between and within networks across the whole brain (i.e., the Fisher-Z correlation values between each ROI pairing, both between and within networks). In addition to ROI-level pairwise comparisons, average within and between-network RSFC comparisons were conducted to assess network-level differences.

GPIP Overview

Individual-specific functional parcels were created for each participant using their RSFC data and GPIP. GPIP uses group-averaged RSFC and the 400-parcel, seven-network Schaefer atlas as priors to a Bayesian formulation that iteratively produces functional parcels that are consistent in number and network-affiliation across groups, but with parcel boundaries specific to each participant (Chong et al., 2017; Schaefer et al., 2018). These individualized parcel boundaries provide more accurate BOLD signal classification for each functional parcel studied. Each parcel corresponded to a region in one of seven functional networks described by the Schaefer atlas (Schaefer et al., 2018; see Figure 9), those being the visual network (VIS), somatomotor network (SOM), dorsal attention network (DAN), ventral attention network (VAN), limbic network (LIM), frontoparietal control network (FPC), and default mode network (DMN).

Figure 9

Example of the 400 parcel, seven-network Schaefer atlas.

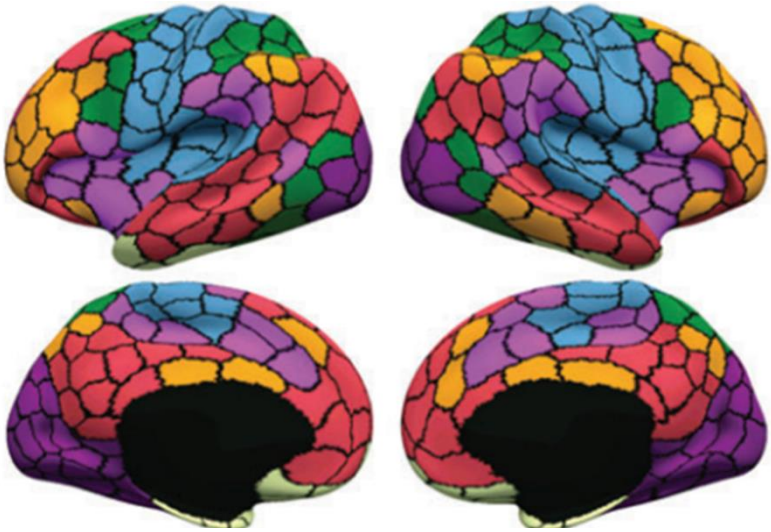

Note. Different colours represent functionally distinct networks, where: purple = VIS, blue = SOM, green = DAN, violet = VAN, cream = LIM, orange = FPC, and red = DMN. Each parcel

represents a functionally distinct region. The RSFC data for each participant in this study were initialized to this atlas, and later refined using GPIP to more accurately define parcel boundaries across individual participants. Schaefer, A., Kong, R., Gordon, E. M., Laumann, T. O., Zuo, X.-N., Holmes, A. J., Eickhoff, S. B., & Yeo, B. T. T. Local-Global Parcellation of the Human Cerebral Cortex from Intrinsic Functional Connectivity MRI. Cerebral Cortex, (2018), 28(9), 3095, by permission of Oxford University Press.

RSFC Data Used

The resulting correlation values for all pairwise parcel-correlations were used to create an RSFC matrix for each participant (see Figure 10). This involved extracting the BOLD timeseries for each voxel, averaging these timeseries across all voxels within each parcel, and calculating the Pearson correlation coefficient between each parcel-pair. Pearson's *r* values were Fisher-Z transformed to standardize the data.

Figure 10

Example of a 400 parcel, seven-network Schaefer atlas ROI-level RSFC matrix.

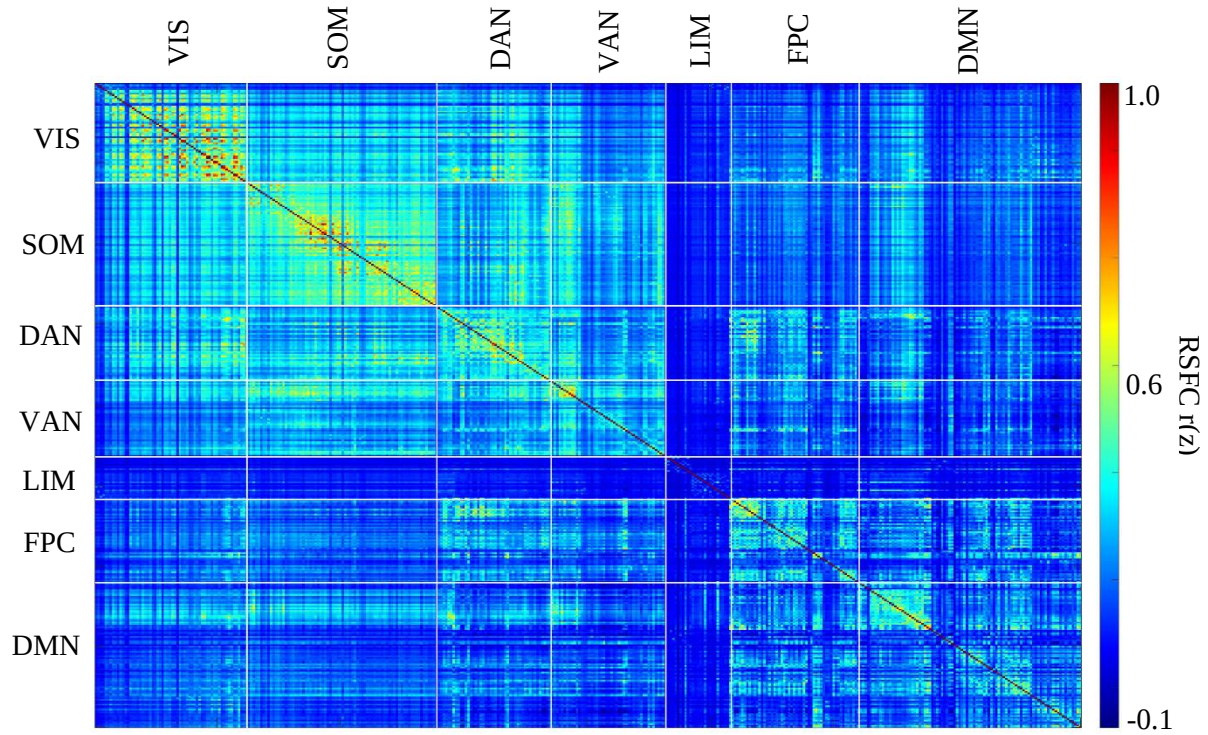

Note. ROI-level RSFC matrices were provided courtesy of Dr. Nathan Spreng. RSFC was measured using the Fisher-Z correlation between the BOLD timeseries of two ROIs. Warm colours indicate strong positive correlation between ROIs, while cool colours represent low/negative correlations between ROIs. RSFC data in these matrices were collected from the first run of rfMRI of the first scan session. These data were used to calculate group average ROI-level and network-level RSFC for each genotype. Network labels: VIS = visual network, SOM = somatomotor network, DAN = dorsal attention network, VAN = ventral attention network, LIM = limbic network, FPC = frontoparietal control network, DMN = default mode network.

Analyses

Univariate analyses were conducted on all pairwise ROI correlations and averaged network level RSFC (that is, the average of all ROI correlations within networks and between different networks). To compare all three genotypes for the Val66Met SNP, a series of Kruskal Wallis-H tests were conducted on all pairwise ROI comparisons and network-level RSFC

comparisons using the seven-network template of the Schaefer atlas (Schaefer et al., 2018). Mann-Whitney U tests were used to compare both pairwise ROI and network-level RSFC between the Val/Val and Met carrier groups. To assess whether the genotype differences in RSFC described by Wang et al. (2014) between the right anterior insular cortex and DLPFC could be observed, an *a priori* analysis based on the findings of Wang et al. (2014) was conducted between these regions. Since the coordinates for the right anterior insular cortex were not provided, and the exact coordinates for the right DLPFC could not be used, the centroid coordinates of these ROIs from the 400 parcel, seven-network Schaefer atlas in MNI space were used (right anterior insula = 40, 6, -16; right DLPFC = 38, 34, 38).

Propensity Score Matching

Propensity score matching (PSM) is a form of subset selection used to create covariate balance between groups so that parametric statistical methods can be employed (D. E. Ho et al., 2011). This allows researchers to use more robust, parametric models to analyze data and, by extension, more confidently interpret findings (D. E. Ho et al., 2007).

Met homozygous participants comprise less than 4% of the full HCP dataset, but due to the large pool of homozygous Val participants I was able to use PSM to compare 14 Val homozygous participants matched on multiple demographic, lifestyle, and cognitive variables to the 14 Met homozygous participants in my sample (D. E. Ho et al., 2007). This analysis was conducted to study the influence of the Met allele on RSFC between the Val and Met homozygous groups, as a means to compare the genotypes where the largest between-group differences are expected.

The R package *MatchIt*, was used to assess the initial imbalance of covariates in an exclusively homozygous dataset (e.g., Val/Val and Met/Mets only) using a general linear model (D. E. Ho et al., 2011). Due to the scope and volume of data collected for the HCP, I was able to match participants on several covariates from demographic (e.g., sex, age, race, handedness, BMI, and zygosity status), lifestyle (e.g., years of education, income, employment, student status, and relationship status), and cognitive domains (e.g., Montreal Mental State Examination (MMSE) score, and Pittsburgh Sleep Quality Index (PSQI) score).

The subset selection implemented by *MatchIt* prunes and weighs "units" (i.e., participants) to produce a weighted subset from the original dataset where BDNF genotype is unassociated with covariates that could act as potential confounds. For the comparison of homozygous Val and Met groups, PSM was used to estimate the average marginal effect of the BDNF genotype on MMSE score while accounting for the potentially confounding covariates mentioned above. After an initial inspection of the imbalances, PSM using 1:1 nearest neighbour and "optimal" approaches were attempted. These matches were unsuccessful at achieving adequate balance for all covariates, so full matching on the propensity score was attempted (Hansen, 2004). I found that using a probit regression of the covariates produced better propensity score estimates compared to logistic regression. See Table 5 for original and matched group means. The distribution of covariates was approximately equal after matching (see Figure 17).

Two sample t-tests were conducted for every unique pairwise ROI correlation in the 400 parcel Schaefer seven-network atlas between the matched Val/Val and Met/Met groups. The average between and within-network RSFC measures for the Schaefer seven-network atlas were also compared using a two-sample t-test for the matched Val/Val group and Met/Met groups.

All analyses were performed using data from the HCP Young Adult dataset through the open access, restricted access, and genetics access data. Analyses were performed in SPSS 28.0 (IBM Corp, 2021), MATLAB R2019b Update 1 (Mathworks Inc., 2019), and R 4.1.3 (R Core Team, 2022). The scripts for GPIP can be requested from the Biomedical Imaging Group of the University of Southern California.

Results

This thesis investigated whether structural differences in CT and functional differences in RSFC were present between healthy young adults according to their genotype for the Val66Met SNP of BDNF. Based on prior observations of reduced CT and decreased RSFC in carriers of the Met allele, I predicted that the Val/Val group would have the greatest CT, followed by the Val/Met group, with the Met/Met group having the lowest CT. Similarly, I predicted that Val/Val participants would have strong functional network integrity, while the Met/Met group would display the weakest network integrity, and the Val/Met group would display network integrity in-between the Val/Val and Met/Met group.

Cortical Thickness

Demographic Statistics

A sample of n = 392 was used to study CT differences. Allele frequencies for the Val66Met SNP were 0.81 and 0.19 for the Val allele and Met allele, respectively. The genotype frequencies of the participant sample were found to be in Hardy-Weinberg equilibrium (Val/Val = 0.65, Val/Met = 0.31, Met/Met = .04; $\chi^2 = 2.70 \times 10^{-3}$, $p = 0.99$). Genotype groups did not differ significantly in age, sex, or education ($p > .05$; see Table 2).

Table 2

Descriptive statistics for the HCP participant subsample used in CT analyses.

Group	n	Mean Age	Male/Female	Mean Years Education
Val/Val	257	28.78 ± 3.72	122/135	15.75 ± 1.86
Val/Met	121	28.00 ± 3.67	54/67	15.09 ± 1.68
Met/Met	14	27.64 ± 5.20	9/5	15.50 ± 1.51
	Total =392	$p = .13^a$	$p = .37^b$	$p = .08^a$

Note. [a]p-value (ANOVA), [b]p-value (Pearson χ^2 test)

Group Comparisons

To assess whether the Val66Met SNP of BDNF influenced structural integrity of the human brain, mean CT differences in 16 ROIs were compared via ANCOVA between all groups, and via Mann-Whitney-U tests to compare Val/Val to Met carriers. An ANCOVA approach was used to covary for possible sex differences that could impact CT (Cieri et al., 2022; Somers et al., 2015; Yang et al., 2020).

The assumption of normally distributed residuals was tested with the Shapiro-Wilk test. Standardized residuals for each ROI were normally distributed across all genotypes and the majority of ROIs ($p > .05$). There was one exception, with the Val/Val group not displaying normally distributed standardized residuals at the left PCC ($W = .84$, $p < 0.001$). Additionally, the assumption of homoscedasticity was also tested, using the Breusch-Pagan Test. Homoscedasticity was observed for all ROIs when comparing between the Val/Val, Val/Met, and Met/Met groups ($p > .05$). However, when comparing between the Val/Val and Met carrier group, the left PCC did violate this assumption ($\chi^2 = 5.53$, $p = .02$). Levene's test was used to test the assumption of homogeneity of variance. Homogeneity of variance was observed for all ROIs when comparing between the Val/Val, Val/Met, and Met/Met groups ($p > .05$) and for most

ROIs when comparing between the Val/Val and Met carrier groups, with the exception of the left IPC (F = 4.74, *p* =.03) and right IPC (F = 5.43, *p* = 0.02).

Of the 16 total ROIs analyzed, nine ROIs had the highest mean CT value (numerically) in the Val/Met group, including the left and right LING, left and right INS, right PG, left and right PCC, right PCUN, and left STG. Mean CT value in the remaining seven ROIs was highest in the Met/Met group, including the left and right IPC, left PC, left PCUN, left and right SFG, and right STG.

Figure 11

Map of the cortical regions investigated for between-group differences in CT.

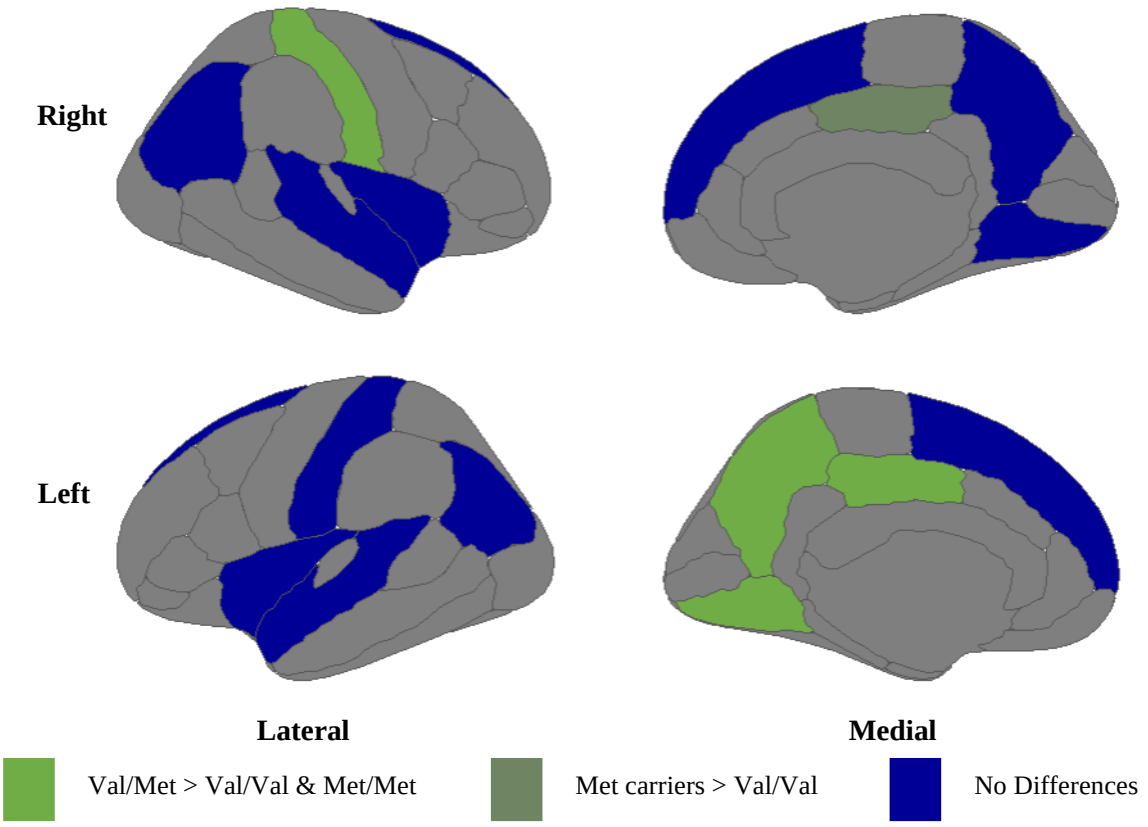

Note. Regions are arranged according to the Desikan Killiany atlas (Desikan et al., 2006). Light green represents regions with signifcant differences with the Val/Met group having the greatest

CT relative to the Val/Val and Met/Met groups (uncorrected p <.05). Muted green represents regions with signifcant differences with the Met carrier group having the greatest CT relative to the Val/Val group (uncorrected p <.05). Regions in blue indicate no significant differences between any genotype groups (uncorrected p >.05).

Comparisons of the Val/Val, Val/Met, and Met/Met groups using ANCOVA revealed a significant difference between the groups at the left PCC, F (2, 391) = 5.40, uncorrected p = .005, and right PCC, F (2, 391) = 3.50, uncorrected p = .03, with the Val/Met group displaying the highest CT at both ROIs, followed by the Val/Met and Met/Met groups (see Figure 13). Post-hoc analyses were performed with a Sidak multiple comparisons correction, which indicated a significant difference between the Val/Val and Val/Met groups for the left PCC (p = .04), but not the right PCC (p = .06) (Sidak, 1967). However, differences in neither of these ROIs survived multiple comparisons correction for false discovery rate (left PCC corrected p = .08, right PCC corrected p = .25; see Table 3). Furthermore, closer inspection of the two ROIs showed that there were outliers for both ROIs that skewed the mean CT of the Val/Val group (see Figure 12).

When the Val/Val and Met carrier groups were compared via Mann-Whitney U test, no significant differences were observed between Val66Met genotypes for the majority of the ROIs (see Figure 14). There were four exceptions where significant differences were initially observed, notably in the left PCC (U = 20272, uncorrected p = .006, rank biserial correlation = .17), right PG (U = 19788, uncorrected p = .02, rank biserial correlation = .14), left PCUN (U = 19708, uncorrected p = .03, rank biserial correlation = .14) and left LING (U = 19550, uncorrected p = .04, rank biserial correlation = .18). In each case, CT was greater in the Met carrier group compared to the Val/Val group. However, differences in none of the ROIs survived multiple comparisons correction for false discovery rate (PCC corrected p = .10; PG corrected p = .14; PCUN corrected p = .14; LING corrected p = .15) (Benjamini & Hochberg, 1995).

Furthermore, closer inspection revealed that several outliers were observed in these ROIs that skewed the mean CT of the Val/Val group (see Figure 12); upon removing these outliers, no signifcant differences were observed ($p > .05$).

Table 3

Mean CT differences between Val/Val, Val/Met, Met/Met, and Met carrier participants.

	Left Hemisphere				Right Hemisphere			
	Val/Val	Val/Met	Met/Met	Met Carriers	Val/Val	Val/Met	Met/Met	Met Carriers
INS								
M	3.1	3.1	3.0	3.1	3.0	3.0	3.0	3.0
SE	.01	.01	.04	.01	.01	.01	.03	.01
Test Statistic		.53[a]		17088[b]		.42		17353.50[b]
p		.73		.86		.73		.99
STG								
M	2.9	2.9	2.9	2.9	3.0	3.0	3.0	3.0
SE	.01	.01	.03	.01	.01	.01	.03	.01
Test Statistic		.39[a]		18065.50[b]		.72		17875.50[b]
p		.73		.72		.73		.75
SFG								
M	2.8	2.9	2.9	2.9	2.9	2.9	2.9	2.9
SE	.01	.01	.03	.01	.01	.01	.03	.01
Test Statistic		.44[a]		18006.50[b]		.25		17816.50[b]
p		.73		.72		.78		.75
IPC								
M	2.6	2.6	2.6	2.6	2.6	2.7	2.7	2.7
SE	.01	.01	.03	.01	.01	.01	.03	.01
Test Statistic		.74[a]		18709.50[b]		1.29		18969.50[b]
p		.73		.36		.63		.28
PCC								
M	2.6	2.6	2.5	2.6	2.5	2.6	2.5	2.6
SE	.01	.01	.04	.01	.01	.01	.04	.01
Test Statistic		5.40[a]		20272[b]		3.50		19373.50[b]
p		.08*		.10*		.25*		.15
PCUN								
M	2.5	2.5	2.6	2.5	2.6	2.6	2.6	2.6
SE	.01	.01	.03	.01	.01	.01	.03	.01
Test Statistic		2.88[a]		19708[b]		1.09		18911.50[b]
p		.30		.14*		.67		.28
PG								
M	2.2	2.2	2.2	2.2	2.2	2.3	2.3	2.3
SE	.01	.01	.03	.01	.01	.01	.03	.01

Test Statistic		1.85[a]		19417.50[b]		1.65		19788[b]
p		.51		.15		.51		.14*
LING								
M	2.2	2.2	2.2	2.2	2.2	2.2	2.2	2.2
SE	.01	.01	.03	.01	.01	.01	.03	.01
Test Statistic		2.44[a]		1955[b]		.48		18545.50[b]
p		.51		.15*		.73		.42

Note. Mean (M), standard error (SE), test statistic and *p* values are reported. [a]ANCOVA was used to compare CT differences between Val/Val, Val/Met, and Met/Met participants, while a [b]Mann-Whitney U test was used to compare between Val/Val and Met carrier groups. Corrected *p* values are reported. ROIs: insula (INS), superior temporal gyrus (STG), superior frontal gyrus (SFG), inferior parietal cortex (IPC), posterior cingulate cortex (PCC), precuneus cortex (PCUN), postcentral gyrus (PG), lingual gyrus (LING). Stars (*) indicate significant differences between groups prior to multiple comparisons correction ($p < .05$), but not after.

Figure 12

Box-and-whisker plots of CT measures (mm) for ROIs with significant uncorrected differences between genotype groups.

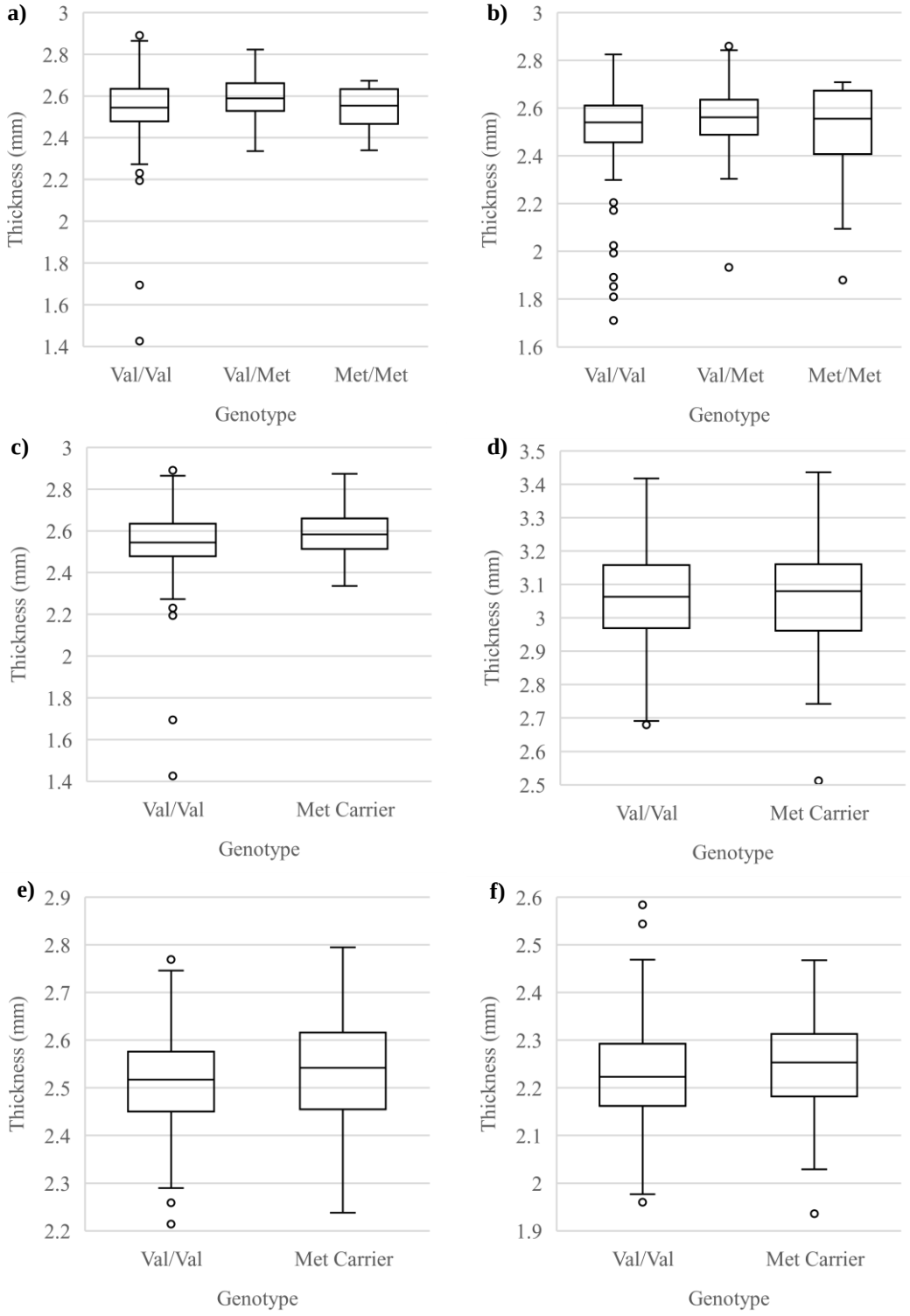

Note. Differences in CT were compared between the Val/Val, Val/Met, and Met/Met groups at

the a) left PCC and b) right PCC, and for the Val/Val and Met carrier groups at the c) left PCC, d) right PC. e) left PCUN, and f) left LING. Whiskers indicate the minimum and maximum values not including outliers, while the box represents the interquartile range between the third and first quartile. The line bisecting the box represents the median CT value. Outliers are represented with the open circles outside of the whiskers; a data point was considered an outlier if it was 1.5 times larger or smaller than the interquartile range.

Figure 13

Mean CT (mm) in the a) left hemisphere and b) right hemisphere between all genotypes.

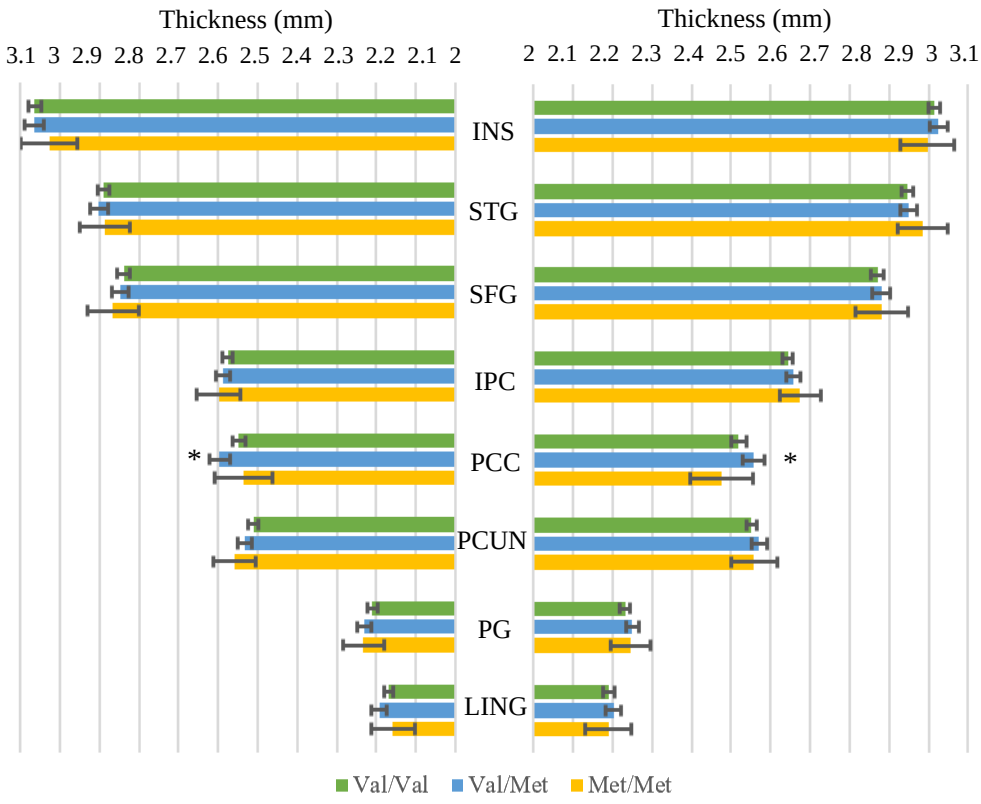

Note. ROIs (vertical axis) were formed using the Desikan-Killiany atlas. Colour bars represent mean CT for Val/Val (green), Val/Met (blue), and Met/Met (yellow) groups, while the error bars represent 95% confidence intervals. The following ROIs were selected based on prior observations of CT differences between Val66Met genotype groups: insula (INS), superior temporal gyrus (STG), superior frontal gyrus (SFG), inferior parietal cortex (IPC), posterior cingulate cortex (PCC), precuneus cortex (PCUN), postcentral gyrus (PG), lingual gyrus (LING).

Significant differences prior to multiple comparisons correction ($p < .05$) were identified between groups at the left and right PCC, with the Val/Met group having the greatest CT, followed by the Val/Val and Val/Met groups. None of these differences were significant after multiple comparisons correction.

Figure 14

Mean CT (mm) in the a) left hemisphere and b) right hemisphere between Val/Val and Met carriers.

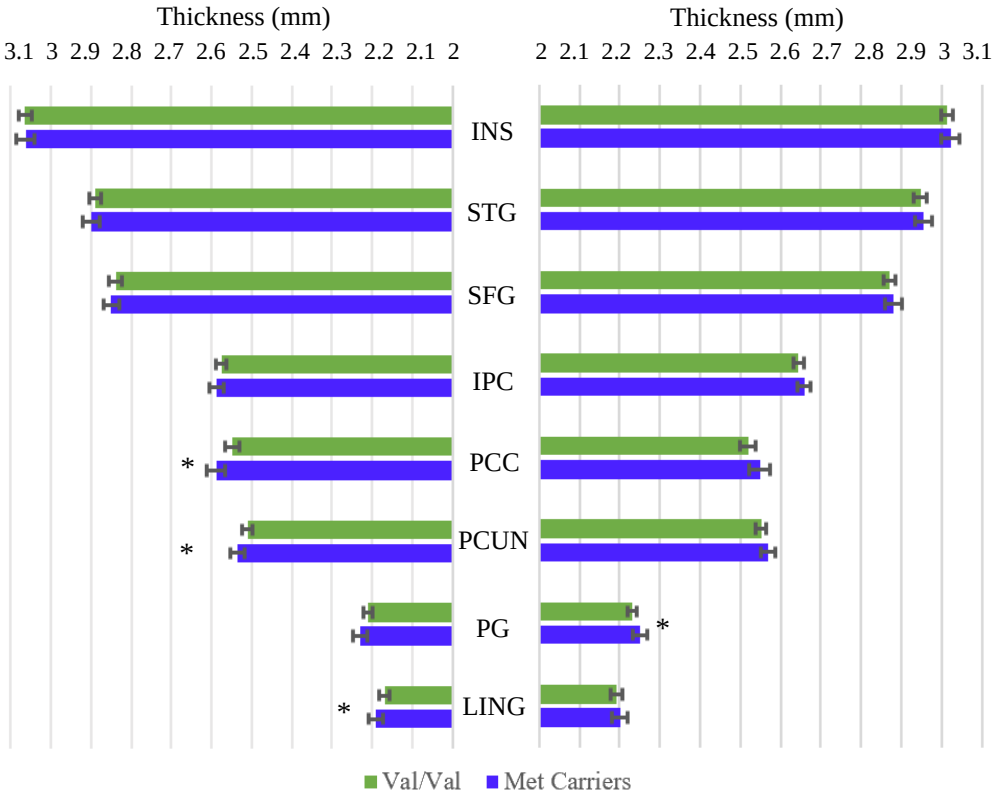

Note. ROIs (vertical axis) were formed using the Desikan-Killiany atlas. Colour bars represent mean CT, while the error bars represent 95% confidence intervals. The following ROIs were selected based on prior observations of CT differences between Val66Met genotype groups: insula (INS), superior temporal gyrus (STG), superior frontal gyrus (SFG), inferior parietal cortex (IPC), posterior cingulate cortex (PCC), precuneus cortex (PCUN), postcentral gyrus (PG), lingual gyrus (LING). Significant differences prior to multiple comparisons correction ($p < .05$) were identified between groups at the left PCC, left PCUN, right PG, and left LING, with the Met carrier group having the greater CT relative to the Val/Val group. None of these

differences were significant after multiple comparisons correction; CT difference in the left PCC approached significance (p = .08).

Resting-State Functional Connectivity

Demographic Statistics

A sample of n = 281 was used to study differences in network function. Allele frequencies for the Val66Met SNP were 0.81 and 0.19 for the Val allele and Met allele, respectively. The genotype frequencies of the participant sample were found to be in Hardy-Weinberg equilibrium (Val/Val = 0.65, Val/Met = 0.31, Met/Met = .04; χ^2 = 1.93, p = 0.38). Genotype groups did not differ significantly in age, sex, or education (p > .05; see Table 4).

Table 4

Descriptive statistics for the HCP participant subsample used in RSFC analyses.

Group	n	Mean Age	Male/Female	Mean Years Education
Val/Val	187	28.75 ± 3.63	87/100	15.17 ± 1.57
Val/Met	80	27.90 ± 3.69	37/43	15.44 ± 1.43
Met/Met	14	27.64 ± 5.20	9/5	15.50 ± 1.51
	Total =281	p = .17[a]	p = .43[b]	p = .34[a]

Note. [a]p-value (ANOVA), [b]p-value (Pearson χ^2 test).

Pairwise ROI Comparisons

A visual inspection of the mean RSFC between all pairwise ROI comparisons revealed typical network structure/organization for the Val/Val, Val/Met, and Met/Met groups in the seven-network model of the 400 parcel Schaefer atlas (see Figure 15; Schaefer et al., 2018).

Three-way Kruskal-Wallis non-parametric tests were conducted to compare RSFC between all pairwise correlations (using the seven-network model of the Schaefer atlas) for Val/Val, Val/Met, and Met/Met groups for the Val66Met SNP. Additionally, all pairwise

correlations were also compared between the Val/Val and Met carrier groups through Mann-Whitney U tests. Although mean RSFC did differ numerically between genotype groups, differences were not statistically significant between groups ($p > .05$; see Figure 15). Furthermore, a targeted analysis of RSFC between the right anterior insular cortex and the right DLPFC based on the *a priori* findings of Wang et al. (2014) did not reveal any significant differences between the Val/Val, Val/Met, and Met/Met groups ($p = .13$) or between the Val/Val and Met carrier groups, although this difference approached significance (U = 10010, $p = .06$). Relative to the Val/Val group, the Met carriers had greater RSFC between the right insular cortex and DLPFC.

Figure 15

Mean RSFC (Fisher-Z correlation) between all pairwise ROIs.

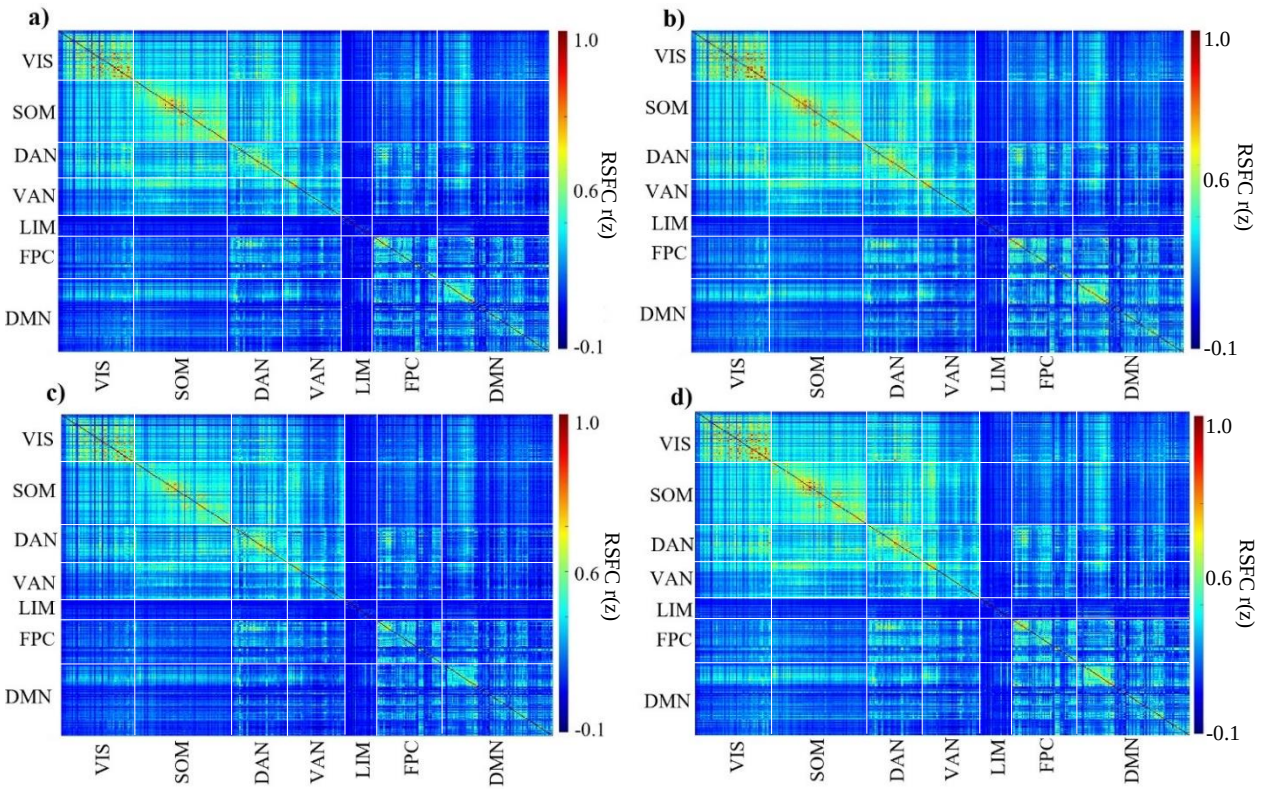

Note. The Fisher-Z correlation was averaged for all participants in the a) Val/Val, b) Val/Met, c) Met/Met, and d) Met Carrier groups to acquire mean RSFC for every pairwise comparison.

Matrices are arranged according to network order of the 400 parcel, seven-network Schaefer atlas (Schaefer et al., 2018). Warm colours indicate strong positive correlation between ROIs, while cool colours represent low/negative correlations between ROIs. Matrices are arranged according to network order of the seven-network Schaefer atlas, where: VIS = visual network, SOM = somatomotor network, DAN = dorsal attention network, VAN = ventral attention network, LIM = limbic network, FPC = frontoparietal control network, DMN = default mode network.

Between and Within-Network Comparisons

Three-way Kruskal-Wallis H non-parametric tests were conducted to perform a network-level comparison of mean RSFC between and within-networks using the seven-network model of the Schaefer atlas (Schaefer et al., 2018) for Val/Val, Val/Met, and Met/Met groups for the Val66Met SNP. All groups demonstrated higher RSFC within networks than between networks. Relative to the Val/Val and Val/Met groups, the Met/Met group displayed the greatest RSFC both within and between networks. Additionally, all network-level correlations were also compared between the Val/Val and Met carrier groups through Mann-Whitney U tests. Again, both groups demonstrated higher RSFC within networks than between networks. The Met carrier group displayed the greatest RSFC between and within networks compared to the Val/Val group.

Results of the Kruskal-Wallis H test did not reveal any significant differences in RSFC between or within-networks among the Val/Val, Val/Met, and Met/Met groups, so no post-hoc comparisons were conducted ($p > .05$; see Figure 16 and 17). The Mann-Whitney U test did not reveal significant differences between the Val/Val and Met carrier groups ($p > .05$), although the difference between these two groups within the DAN approached significance ($U = 9905$, $p = .08$; see Figures 16 and 17), with the Met carrier group displaying greater RSFC within the DAN than the Val/Val group.

Figure 16

Comparison of network-averaged RSFC between- and within-networks.

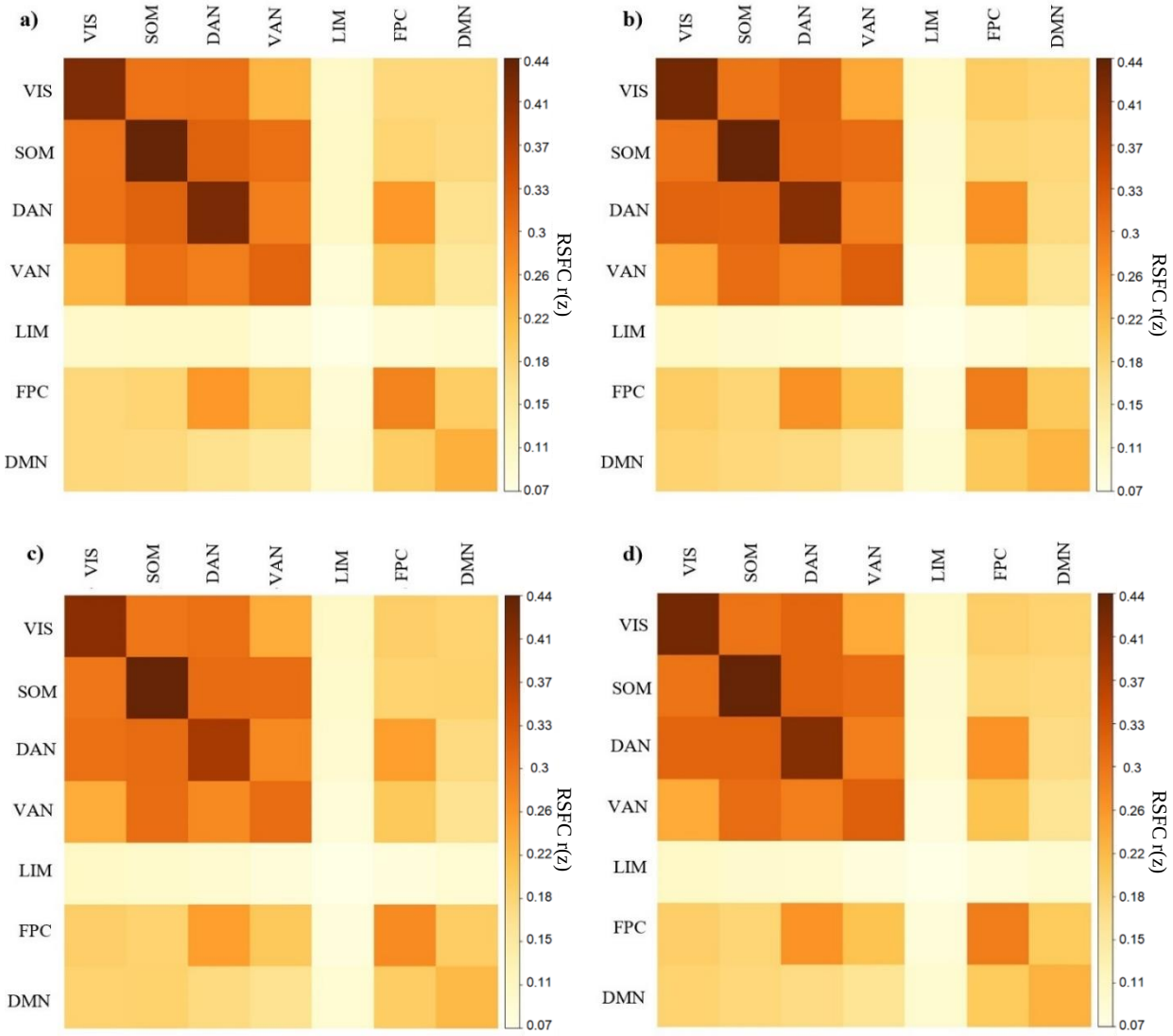

Note. Mean RSFC was calculated using the mean Fisher-Z correlation between each ROI pair both between and within-networks atlas for the a) Val/Val group, b) Val/Met group, c) Met/Met group, and d) Met carrier group. Darker colours represent higher RSFC, while brighter colours represent lower RSFC. Matrices are arranged according to network order of the 400 parcel, seven-network Schaefer atlas (Schaefer et al., 2018), where: VIS = visual network, SOM = somatomotor network, DAN = dorsal attention network, VAN = ventral attention network, LIM = limbic network, FPC = frontoparietal control network, DMN = default mode network.

Figure 17

Test statistics (left) and significance values (right) of network-averaged RSFC comparisons.

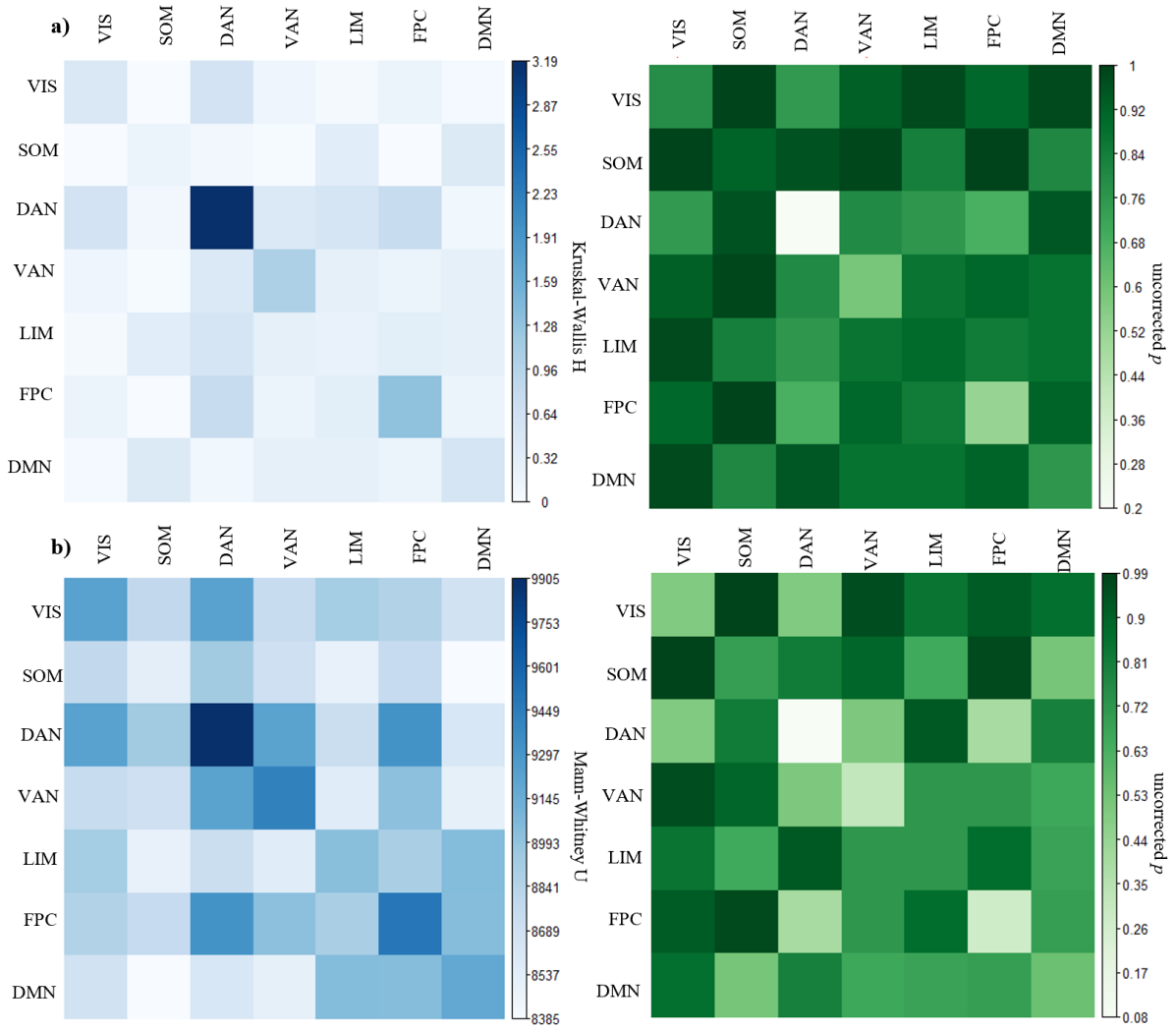

Note. Test statistics were calculated using the Kruskal-Wallis H test and Mann-Whitney U test for the comparisons a) Val/Val, Val/Met, and Met/Met groups, and b) Val/Val and Met carrier groups, respectively. Darker shades of blue on the test statistic matrix indicate greater between group differences, while darker shades of green on the uncorrected *p* matrix indicate values further from significance. Matrices are arranged according to network order of the 400 parcel, seven-network Schaefer atlas (Schaefer et al., 2018), where: VIS = visual network, SOM = somatomotor network, DAN = dorsal attention network, VAN = ventral attention network, LIM = limbic network, FPC = frontoparietal control network, DMN = default mode network.

Differences between groups were typically small in both the comparisons, although the difference between the Val/Val and Met carrier groups within the DAN was large and approached significance (p = .08).

Smaller Sample Comparisons Following PSM

PSM allows one to create individually matched groups of participants based on multiple covariates. The goal of PSM in this study was to evaluate whether comparing Val/Val and Met/Met groups of equal sample sizes of better-matched participants across multiple variables would produce similar results to the previous analysis with a larger, unmatched Val/Val group. PSM was used to identify 14 Val/Val participants optimally matched with the Met/Met participant sample (n=14) on various demographic, lifestyle, and cognitive measures. Propensity scores for each of the matched groups are plotted in Figure 16. Following PSM, the group sizes were 14 Val/Val participants (age: mean ± SD = 27.38 ± 4.79 , 5 female) and 14 Met/Met participants (age: mean ± SD = 27.64 ± 5.20 , 5 female).

Table 5

Covariate Balance across Met/Met and Val/Val groups before and after matching on the Propensity Score.

	Original Sample					Matched Sample				
Variable	Met Mean (n=14)	Val Mean (n=708)	Std Mean Difference	Test Statistic	p	Met Mean (n=14)	Val Mean (n=14)	Std Mean Difference	Test Statistic	p
MMSE	28.71	29	-.40	3743[a]	.10	28.71	28.65	.09	-.43[c]	.67
Sex				2.55[b]	.12				0[b]	1
Female	5	406	-.45			5	5	.07		
Male	9	302	.45			9	9	-.07		
Age	27.64	28.90	-.24	4006[a]	.22	27.64	27.38	.05	-.61[c]	.55
Race				28.18[b]	0.003				0[b]	1
Amer. Indian	0	0	-.05			0	0	-.01		

Asian	.29	.03	.56			.29	.29	-.01		
Black	0	.20	-.50			0	0	-.01		
Two or more	0	.03	-.17			0	0	-.02		
Not reported	0	.02	-.14			0	0	-.01		
White	.71	.72	-.02			.71	.71	-.01		
Handedness	67.86	67.27	.01	4791.50[a]	.83	67.86	66.50	.03	-.03[c]	.98
Zygosity				1.02[b]	.60				2.29[b]	.32
MZ twin	.43	.31	.24			.43	.30	.26		
DZ twin	.14	.21	-.19			.14	.19	-.14		
Not twin	.43	.48	-.11			.43	.51	-.17		
Education	15.50	14.79	.47	6000[a]	.16	15.50	15.55	-.03	-.38[c]	.71
BMI	24.03	26.78	-.55	3271.50[a]	.03	24.03	24.22	-.04	.51[c]	.62
Employment	1.43	1.54	-.13	4682[a]	.67	1.43	1.53	-.12	-.47[c]	.64
PSQI Score	3.93	4.82	-.42	3999[a]	.21	3.93	3.97	-.02	-.54[c]	.59
Income				6.69[b]	.57				3.83[b]	.70
1	.07	.08	-.03			.07	.06	.06		
2	.07	.08	-.05			.07	.07	.01		
3	0	.13	-.39			0	.01	-.04		
4	.14	.13	.04			.14	.10	.11		
5	.14	.08	.17			.14	.19	-.14		
6	.07	.21	-.56			.07	.06	.06		
7	.21	.13	.20			.21	.21	.01		
8	.29	.14	.33			.29	.30	-.03		
Not reported	0	.01	-.08			0	0	-.01		
In school	.21	.19	.06	.05[b]	.82	.21	.25	-.10	0[b]	1
In relationship	.43	.44	-.02	0.00004[b]	.94	.43	.44	-.02	.14[b]	.70
Cocaine use	0	0	-.05	.04[b]	.84	0	0	-.01	0[b]	1
THC use	.07	.13	-.22	.39[b]	.53	.07	.08	-.04	1.17[b]	.28

Total alcohol/week	3.36	4.70	-.23	4377.50[a]	.44	3.36	3.22	.02	.50[c]	.62

Note. Lower standardized mean differences (closer to 0) indicate less difference between groups on a given variable. Significance tests used were: [a]Mann-Whitney U test, [b]Pearson χ^2 test, [c]Student's t-test. Variables used in the PSM analysis are listed in the first column, and include: Mini Mental State Exam (MMSE) score, sex, age, self identified race (American Indian, Asian, Black, Two or more, Not Reported, White), years of education, Body Mass Index (BMI), employment status, Pittsburgh Sleep Quality Index score, total household income (<$10,000 = 1,10K-19,999 = 2, 20K-29,999 = 3,30K-39,999 = 4, 40K-49,999 = 5, 50K-74,999 = 6, 75K-99,999 = 7, >=100,000 = 8), enrollment in school at time of testing, relationship status, positive test for cocaine use on any day of testing, positive test for THC use on any day of testing, and total number of alcoholic beverages per week.

Figure 18

Standardized mean differences for selected covariates before (red) and after (blue) PSM

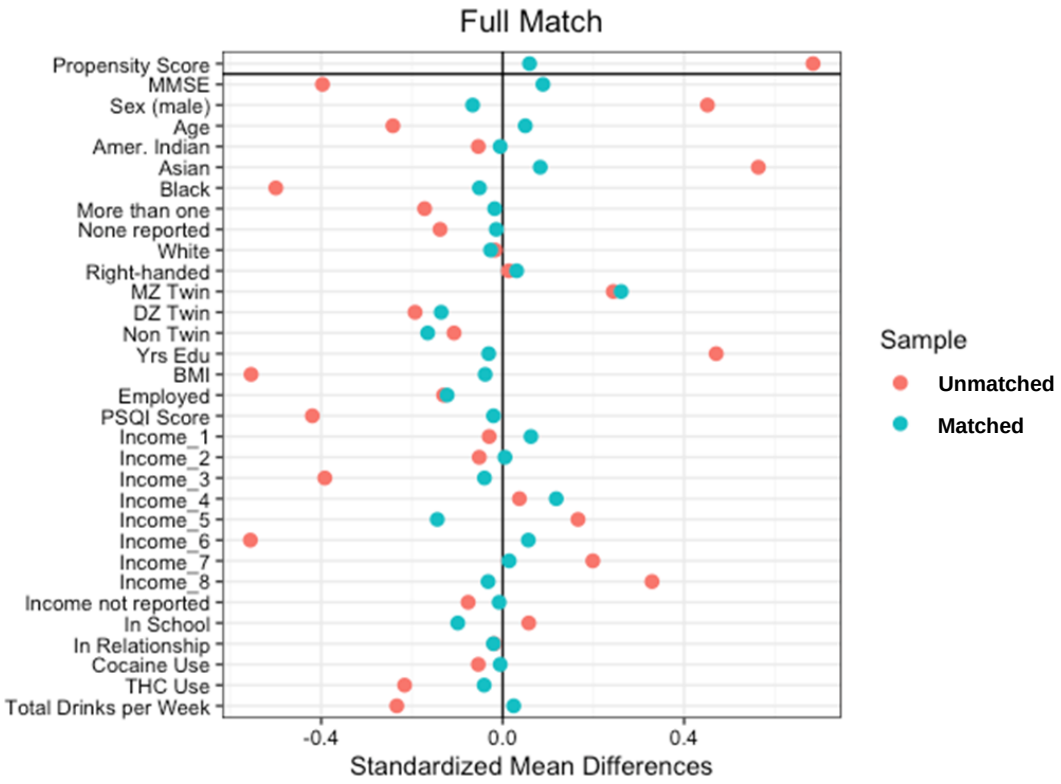

Note. The vertical centre line indicates no standardized mean differences between the Met/Met group and the unmatched (red) or matched (blue) Val/Val groups. Lower standardized mean differences (closer to 0) indicate less difference between groups on a given variable. Variables used in the PSM analysis are listed in the first column, and include: Mini Mental State Exam (MMSE) score, sex, age, self identified race (American Indian, Asian, Black, Two or more, Not Reported, White), years of education, Body Mass Index (BMI), employment status, Pittsburgh Sleep Quality Index score, total household income (<$10,000 = 1,10K-19,999 = 2, 20K-29,999 = 3,30K-39,999 = 4, 40K-49,999 = 5, 50K-74,999 = 6, 75K-99,999 = 7, >=100,000 = 8), enrollment in school at time of testing, relationship status, positive test for cocaine use on any day of testing, positive test for THC use on any day of testing, and total number of alcoholic beverages per week.

Using PSM to identify 14 Val/Val participants matched to the 14 Met/Met participants, a series of independent samples t-tests were conducted to compare RSFC between all pairwise ROI interactions between these groups. Following correction for multiple comparisons (false discovery rate; Benjamini & Hochberg, 1995), no significant differences in RSFC between any pairs of ROIs were identified between the groups (corrected $p > .05$; see Figure 19). A targeted analysis of RSFC between the right anterior insular cortex and the right DLPFC based on the *a priori* findings of Wang et al. (2014) did not reveal a significant difference between the PSM matched Val/Val, and Met/Met groups ($p = .79$)

Figure 19

Mean RSFC (Fisher-Z correlation) between all pairwise ROIs for the: a) PSM Val/Val and b) Met/Met groups.

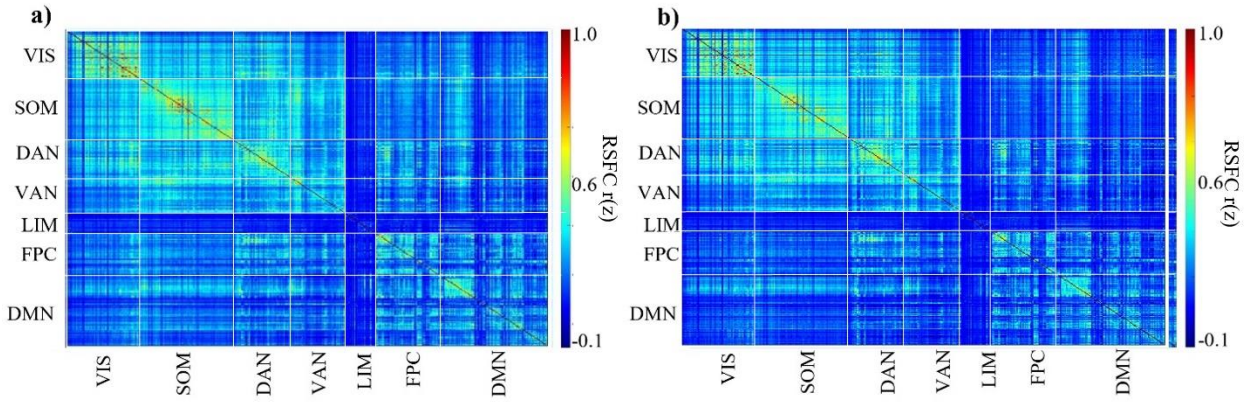

Note. The Fisher-Z correlation was averaged for all participants in the a) PSM matched Val/Val and b) Met/Met groups to acquire mean RSFC for every pairwise comparison. Matrices are arranged according to network order of the 400 parcel, seven-network Schaefer atlas (Schaefer et al., 2018). Warm colours indicate strong positive correlation between ROIs, while cool colours represent low/negative correlations between ROIs. Matrices are arranged according to network order of the seven-network Schaefer atlas, where: VIS = visual network, SOM = somatomotor network, DAN = dorsal attention network, VAN = ventral attention network, LIM = limbic network, FPC = frontoparietal control network, DMN = default mode network.

Mean RSFC between and within functional networks using the seven-network Schaefer atlas was also evaluated for the PSM-matched samples. Both the PSM Val/Val and Met/Met groups demonstrated higher RSFC within networks than between networks. Relative to the PSM Val/Val group, the Met/Met group displayed the greatest RSFC within and between networks. RSFC values for PSM Val/Val and Met/Met groups were not significantly different between any within or between network comparisons ($p > .05$; see Figures 20 and 21).

Figure 20

Comparison of network-averaged RSFC between- and within-networks for the a) PSM Val/Val and b) Met carrier groups.

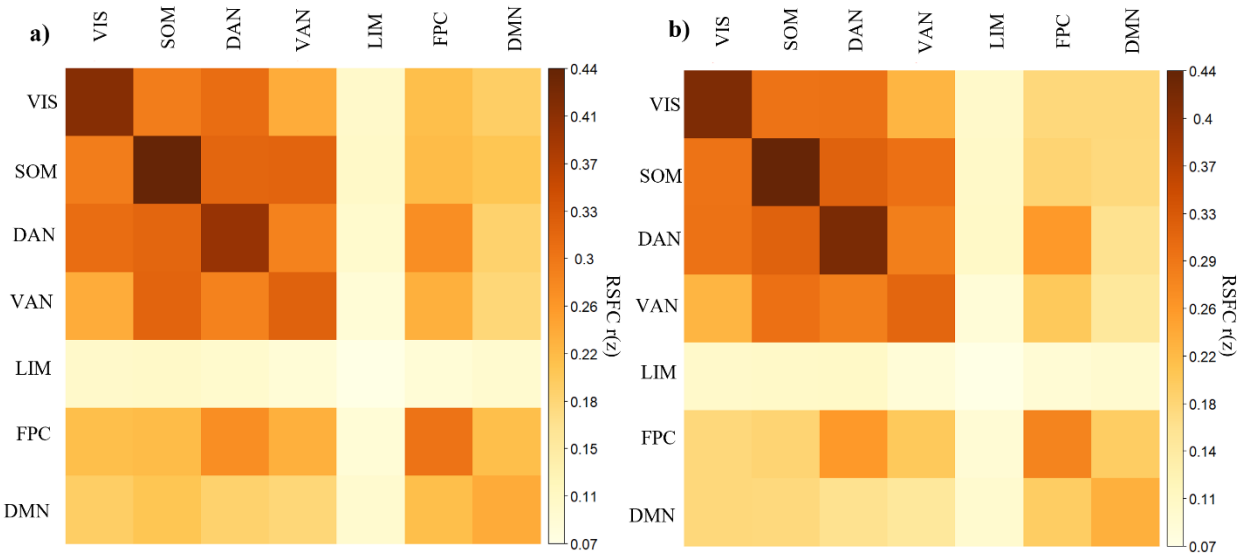

Note. Mean RSFC was calculated using the mean Fisher-Z correlation between each ROI pair both between and within-networks. Darker colours represent higher RSFC, while brighter colours represent lower RSFC. Matrices are arranged according to network order of the seven-network Schaefer atlas, where: VIS = visual network, SOM = somatomotor network, DAN = dorsal attention network, VAN = ventral attention network, LIM = limbic network, FPC = frontoparietal control network, DMN = default mode network.

Figure 21

Test statistics (left) and significance values (right) of network-averaged RSFC comparisons between the PSM matched Val/Val and Met/Met groups.

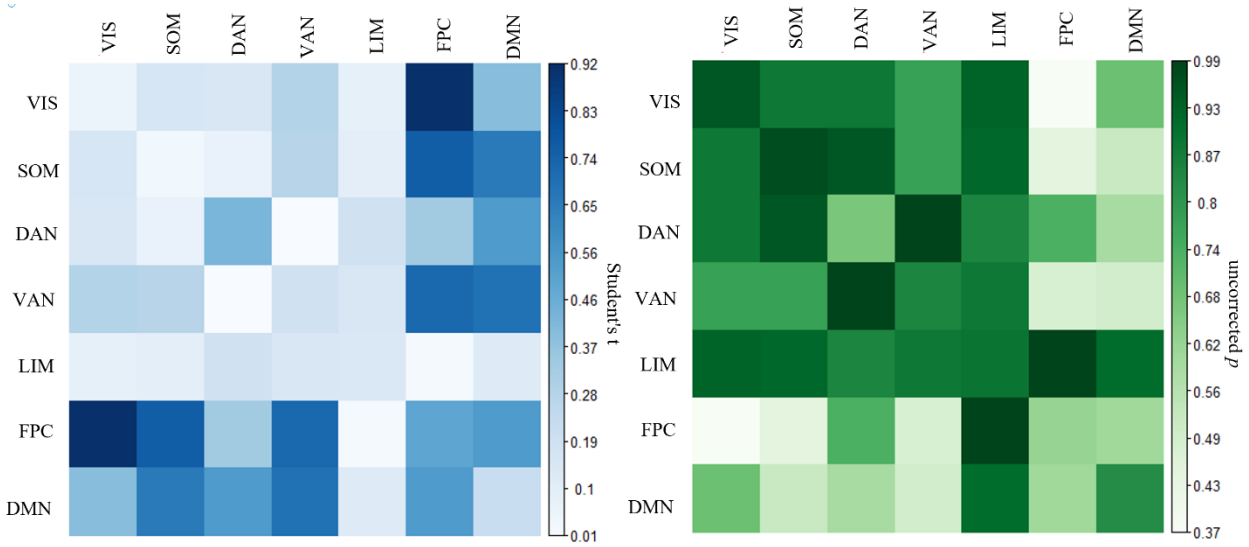

Note. Test statistics were calculated using a Student's t-test. Mean RSFC was calculated using the mean Fisher-Z correlation between each ROI pair between and within-networks. Darker shades of blue on the test statistic matrices indicated greater between group differences, while darker shades of green on the uncorrected *p* matrices indicated values further from significance. Matrices are arranged according to network order of the seven-network Schaefer atlas, where: VIS = visual network, SOM = somatomotor network, DAN = dorsal attention network, VAN = ventral attention network, LIM = limbic network, FPC = frontoparietal control network, DMN = default mode network.

Discussion

The Val66Met SNP of the BDNF gene has been studied in the context of cellular level changes to dendritic outgrowths (Chen et al., 2004; Egan et al., 2003) and in neurodegenerative and psychiatric diseases, such as schizophrenia, major depressive disorder, and Alzheimer's disease (Egan et al., 2003; Hosang et al., 2014; Lim et al., 2021). Notably, differences in CT and RSFC in healthy carriers of the Met allele for this SNP have previously been reported, suggesting that cellular-level effects of the Met allele may impart a deleterious effect on the structural and functional integrity of the brain (Jang et al., 2012; Jasínska et al., 2017; Thomason et al., 2009; C. Wang et al., 2014; X. Yang et al., 2012).

However, previous efforts to study the neurological implications of carrying the BDNF Met allele faced two considerable challenges. Previous studies have been limited by small sample sizes (range of total participants: 32-78 participants in CT studies, 23-38 participants in RSFC studies, with the Wang et al. (2014) study being the exception for both study types), and due to the low prevalence of the Met/Met genotype, these participants were often grouped with the Val/Met participants. Additionally, neuroimaging methods have progressed alongside technological and theoretical advances since these earlier studies, expanding the ways in which empirical questions can be addressed and data can be analyzed. To avoid previous limitations, this study used a comparatively large sample of participants from the HCP, combined with a cutting-edge functional parcellation method (GPIP), to evaluate whether the Val66Met SNP has an impact on CT and RSFC on a population of North American healthy young adults. I hypothesized that the Val/Val group will show the highest structural integrity (i.e., highest CT), followed by the Val/Met and Met/Met groups who carry the potentially deleterious Met allele. I predicted a similar pattern with respect to RSFC, where the Val/Val group will show higher

network integrity (i.e., robust differentiation of functional network structure) than the Val/Met group, and both Val/Val and Val/Met groups higher than the Met/Met group (see Figure 6). Here, I demonstrate that there were no significant differences in CT or RSFC in healthy young adults who differed by genotype for the Val66Met SNP of BDNF.

Cortical Thickness of Val66Met Genotypes

Differences in CT are expected to provide insight into structural integrity at the level of the columnar organization of the neocortex. Neuron columns are important functional units in the neocortex, and reductions in CT could suggest impacts to the structure or number of neurons in a column. Although the parcels of the Desikan-Killiany atlas cover fairly large areas relative to other brain parcellations (e.g., 400 parcel Schaefer atlas), the reduction of neurons in column(s) within a given ROI would be reflected as a change in CT. The following section will describe the analysis, how these results relate to previous findings, and alternative neuroimaging approaches that could be utilized to study cortical thickness.

ROI Analysis

The mean CT of eight ROIs in each of the left and right hemispheres of the neocortex were compared between genotypes for the Val66Met SNP of BDNF in a sample of 392 participants. These ROIs were selected due to previous studies of CT differences between genotype groups and their relationships with intrinsic functional networks, including the DMN and FPC, where RSFC differences have been identified between Val/Val and Met carriers (Jang et al., 2012; Thomason et al., 2009). No consistent or significant differences were observed between the Val/Val, Val/Met, and Met/Met groups when sex was included as a covariate, nor between Val/Val and Met carriers. Based on the absence of CT differences between genotypes, I

do not expect that the structural integrity of neuron layers is impacted, although microscale cellular differences cannot be ruled out, as they are not directly shown by CT measures.

Yang et al. (2012) did observe between-group differences in CT in a sample of Han Chinese healthy young adults. In that study, the Val/Val (n = 15) participants consistently had significantly greater thickness in various regions, including the INS and PCC, relative to the Met/Met group (n = 17), and greater thickness in the PC and INS relative to the Val/Met (n = 29) group. Not long after, Wang et al. (2014) reported no significant differences in CT between Val/Val (n = 95), Val/Met(n = 156), and Met/Met(n = 57) groups of the SNP in a healthy population of Han Chinese young adults (n = 308, female = 166), despite observing differences in RSFC between genotype groups. The reason for these contradictory results is unclear, as both studies used the same methodological approach to measure CT. Some possible explanations could include the stricter exclusion criteria and smaller sample sizes in the study by Yang et al. (2012) or that sex was not controlled for by Wang et al. (2014). A replication study of the latter should be conducted on the Han Chinese population, with more efforts to covary for CT impacting factors including sex to get a better understanding on the role of Val66Met on CT. Although this study was conducted in a North American population of mostly Caucasian participants, the comparatively larger sample sizes used in the present study and by Wang and colleagues seem to indicate that healthy young adult brains are not susceptible to CT differences based on the Val66Met SNP alone (Wang et al., 2014).

Interestingly, a relationship between the developing brain and the BDNF Met allele has been observed. While the influence of the Met allele on CT varied in different studies of healthy young adults, studies in healthy children have shown a consistent difference by genotype group for the Val66Met SNP. In a group of healthy 6 to 10-year-olds, Jasińska et al. (2017) observed

greater thickness in the left STG, temporal pole, and entorhinal cortex for the Val/Val relative to Met carriers, and greater thickness in Met carriers relative to Val/Val in regions including the left PC and the right LING. In typically developing children ages 6-12 years old, de Araujo et al. (2018) found increased CT in the lateral occipital cortex for Met carriers relative to the Val/Val group, while greater CT for Met carriers was observed in the right middle temporal gyrus in a group of children ages 6-12-years old diagnosed with various psychiatric disorders including but not limited to major depressive disorder, bipolar disorder, autism, anorexia nervosa, among many others. It remains unclear why previous work showed predominantly greater CT for Met carriers and Met homozygotes relative to Val homozygotes since the Met allele is typically considered deleterious based on the effects it has at the cellular level. It is possible that the increase in CT for Met carriers is the result of compensatory mechanisms from other neurotrophins. This difference should be explored further in children determine the age/developmental stage at which BDNF genotype-based differences in CT cease to be significant.

Alternative Methods to Measure Structural Integrity

BDNF is also thought to contribute to myelinogenesis — the process by which axons are myelinated for faster action potential conduction — as well as the regeneration of myelin following injury (Du et al., 2003; Fletcher et al., 2018). These two functions may be impacted by the Val66Met SNP, where the Met allele may not allow for these pathways to be properly engaged. Therefore, other neuroimaging methods such as diffusion tensor imaging (DTI) might provide insightful comparisons of white matter integrity between genotypes. Previous DTI studies aiming to identify the structural effects of this SNP have displayed inconsistent results. Some studies of healthy adults suggest greater white matter integrity in Met carriers (Tost et al., 2013), while others report decreased white matter robustness in Met carriers (Carballedo et al.,

2012; C. Park et al., 2017) Although these studies had generally larger sample sizes than other CT studies (range: 42-85 participants), each study grouped the Val/Met and Met/Met participants into a Met carrier group, so differences between Val/Met and Met/Met individuals have not been studied. Additionally, the number of Met carriers varied drastically between studies (e.g., 8 Met carriers of 42 total participants in Tost et al. study, 55 Met carriers of 73 total participants in Park et al. study), making it difficult to draw accurate conclusions on the influence of this SNP on white matter integrity. Future studies on white matter differences between genotypes for BDNF Val66Met should aim to expand the sample size of participants recruited and to evaluate differences between all three genotypes with more evenly balanced groups.

Altogether, this study did not show CT differences in the eight bilateral ROIs studied between the Val/Val, Val/Met, Met/Met, or Met carrier groups of healthy young adults. While these results did not support my hypotheses of structural integrity differences between genotypes, they are consistent with another study that had a similar group size (C. Wang et al., 2014), but inconsistent with findings in studies with smaller sample sizes (X. Yang et al., 2012) and in studies of children (de Araujo et al., 2018; Jasínska et al., 2017). Further research on other measures of structure, including white matter integrity, should be conducted to gather a complete picture of the effects of the Val66Met SNP on structure.

Resting-State Functional Connectivity

While previous studies have reported differences in RSFC between BDNF genotypes, this study, which used larger sample sizes and more advanced, rigorous analysis techniques, did not replicate any of the aforementioned findings. After examining pairwise ROI comparisons using the 400-parcel, seven-network Schaefer atlas, as well as averaged within and between-network connectivity, I did not observe any significant differences in RSFC between the

Val/Val, Val/Met, and Met/Met groups, or when grouping Met carriers together. This was true of both a large sample comparison comprising 281 participants and a smaller PSM group comparison of 28 participants, comprising 14 Val/Val and 14 Met/Met participants.

Typical Functional Connectivity Between Genotypes

Across all the genotype groups studied, typical functional integrity of intrinsic functional networks was observed: the highest RSFC correlations were within network, while between-network measures were comparatively lower. At the pairwise comparisons level, ROIs close to the diagonal (i.e., ROIs of the same network) had the highest Z-scores. ROIs were less correlated as comparisons moved away from the diagonal (i.e., comparisons between networks). The same pattern was observed for RSFC measures when averaging all pairwise comparisons between and within-networks. While I predicted that there would be between-groups differences in inter- and intra-network RSFC, the results show typical functional integrity of intrinsic functional networks. These results contradict the within-network decreases in networks like the DMN and FPC for Met carriers (Jang et al., 2012; Thomason et al., 2009), as well as increasing RSFC between the anterior insula and DLPFC in a dosage-dependent manner, such that the highest RSFC correlation was observed in the Met/Met group, followed by the Val/Met group, and lastly the Val/Val group (C. Wang et al., 2014).

Improving Statistical Power with Larger Samples

The sample of 281 participants used in this study represents the largest sample used to study RSFC in relation to the Val66Met SNP. Until now, the largest sample in a study of RSFC differences between genotypes for Val66Met was that of Wang et al. (2014), with a sample of 280 participants. Thomason et al. (2009) recruited a sample of 38 participants, and Jang et al. (2012) had a sample of 23 participants. While these are typical sample sizes for a neuroimaging

study, Marek and colleagues (2022) have recently argued that much larger sample sizes are required to reduce the likelihood of spurious correlations when investigating brain-behaviour relationships. They analyzed the three largest neuroimaging datasets available and found that the median sample size used (n = 25) was unlikely to replicate in a separate sample. Additionally, studies with smaller sample sizes also reported larger effect sizes (e.g., 0.2 or greater), while the large-sample replications reported a 0.01 median effect size (Marek et al., 2022). This study illustrates the importance of sample size in neuroimaging studies; researchers should strive to recruit larger samples and continue to work with large neuroimaging datasets as a means to ascertain the validity of findings with smaller samples.

Methodological Considerations in RSFC Analysis

Among the many methodological decisions to be made in group-level rfMRI analyses, two in particular can influence results substantially, sometimes introducing error and/or bias, including 1) the atlas used (e.g., atlases are often based on cellular structure), and 2) the seed-based correlation method used to identify ROIs and, by extension, intrinsic functional networks.

Atlases are not Specific to Individuals

It is typical for both anatomical and functional data to be spatially aligned to a common atlas that represents averaged anatomical/functional boundaries for the population being studied (Gholipour et al., 2007; Schaefer et al., 2018; Yeo et al., 2011). To illustrate, a study comparing younger and older participants would require an atlas created using both age-groups to best fit the data and avoid biasing the results in favour of either group. While group-averaged atlases enable comparisons at the group level in a straightforward manner and the number of available atlases continues to expand (e.g., older adults, clinical populations), even the best atlas cannot fully account for individual differences in structural and functional topology. Registering all

participants to a common template may fail to identify or correctly characterize the relationship/connectivity between functional regions (Gordon et al., 2015; Mueller et al., 2013; D. Wang et al., 2015). Furthermore, these atlases are often based on structural properties of the brain, despite observations that structural and functional boundaries often do not correspond (Suárez et al., 2020). Methods like GPIP are becoming the new standard in neuroimaging studies because they mitigate these shortcomings by creating accurate functional parcels for each participant using the participant's RSFC data, while employing the most up-to-date functional atlases as biological constraints (Chong et al., 2017). Using individualized parcellation methods can improve the accuracy of RSFC measurements across groups, allowing for researchers to observe potentially novel findings that were previously undetected by methods that obscured the nuances of dynamic relationships between low frequency signals (Chong et al., 2017). Equally relevant is the opportunity to use more precise methods of measuring RSFC to test the strength and significance of previously reported effects through data reanalysis and replication studies.

Seed-based Correlational Analyses are not Always Accurate

The second issue, seed-based correlation methods for quantifying RSFC, may also introduce errors into analyses. In this approach, the rfMRI signal of a specific coordinate-based location (the "seed") is correlated with the timeseries of other brain regions or the rest of the brain (Biswal et al., 1995; Fox et al., 2005). This method requires the seed to be determined beforehand, often using coordinates identified by other researchers in the literature (e.g., coordinates of the voxel with peak activation during task fMRI, or from strictly anatomically based definitions). This method also assumes that functional regions are consistent between participants when mapped onto a template/atlas used for group analysis. However, the choice of seed may not accurately reflect an interaction between large scale brain networks, which can lead

to variability in results within and between studies (Glezer & Riesenhuber, 2013; Kerepesi et al., 2018; Sohn et al., 2015). Furthermore, seeds are often defined as a sphere, wherein the average timeseries of all voxels within that sphere are correlated with the rest of the brain. The process of selecting seed size is arbitrary, does not necessarily reflect the actual size or shape of the ROI, may capture timeseries from voxels that are not part of the functional region of interest, and may not reflect individual differences in functional connectivity (Cole et al., 2010).

The Importance of Individual Localization to Functional Neuroimaging

A study by Glezer and Reisenhuber (2013) showed that the location of functional activation of a region, such as the visual word form area (VWFA), can vary considerably between participants, literature coordinates, and even the group average of all participants in a sample. In their study, differences between the location of an individual's VWFA and the group-averaged or literature-based VWFA were so large that using either group- or literature-based coordinates as seeds did not reveal any specificity for words in the VWFA, an area which is known to be specialized for processing written words. This points to the necessity of individualized functional parcellations of the brain when studying RSFC, especially at the group-level, since the seed-based approach alone cannot accommodate the variance in ROI location across individuals.

Literature Coordinates Based are Insufficient

Previous studies of RSFC and the Val66Met SNP have used literature-based seed-based comparison. In the original paper that identified RSFC differences between genotype groups for Val66Met, Thomason et al. (2009) used literature-based coordinates for the three networks they evaluated (DMN, right PCC: 10, −50, 30; FPC, right DLPFC: 44, 36, 20; Salience Network,

right pars orbitalis : 38, 26, −10; MNI coordinates used) and found within-network RSFC differences in children who were carriers of the Met allele, relative to Val/Val children. Thomason's group (2009) reported that Met carriers had reduced within-network RSFC for the DMN and FPC and increased within-network RSFC for the paralimbic network. This was also the case in the study of young adults by Jang et al. (2012), where literature-based coordinates for the left PCC (-5, -49, 40) were used to seed intrinsic functional networks. They observed RSFC differences between the PCC and precuneus, such that Met carriers showed a weaker relationship between the two nodes compared to the Val/Val group. While it is not inherently incorrect to use seeds, neither of these studies accounted for the individual differences in the locations of functional regions between participants because they apply the literature coordinates to each participant.

The Choice of Seed Can "Beg the Question"

Wang et al. (2014) obtained their RSFC seed using the ROI where they reported significant group differences for cortical surface area (the insular cortex). It can be the case that CT differences can inform structural connectivity differences. Indeed, one of the first papers to show small world connectivity of anatomical networks in humans, a theory that is widely accepted today as the way the brain is anatomically organized, did so by assessing CT associations between areas (He et al., 2007). Others, (e.g., Lerch et al., 2006) have shown direct differences in CT that impact anatomical connectivity through diffusion tensor imaging. Although studies have shown that structural connectivity can sometimes predict functional connectivity (Honey et al., 2009), functional connectivity represent dynamic interactions between regions that are subject to changes over short periods of time (e.g., milliseconds), making structural connectivity an unreliable measure of the functional relationships between

disparate regions of intrinsic functional networks (Ekman et al., 2012; Hermundstad et al., 2013; Sporns, 2011). Leveraging the debateable assumption that structural and functional connectivity have an isomorphic relationship, Wang and colleagues (2014) chose the right angular gyrus as a seed for RSFC based on cortical surface area differences. This design is circular in that the premise assumes the consequence; that is, they assumed the coordinates where CT differences were identified could be seeded to identify differences in RSFC. Researchers should be careful not to misinterpret the overlap of structural and functional networks since changes on the cortical surface may not necessarily reflect functional changes for either short- or long-range connections. Functional networks are more flexible than structural networks and regional overlap between networks should not be misconstrued as isomorphic (H.-J. Park & Friston, 2013).

There is an increased push in the field of fMRI to adapt methods that create individualized brain parcellations for more accurate assessments of functional connectivity. Other approaches to generating individualized brain parcellations akin to GPIP have been developed using different algorithms (Blumensath et al., 2013; Kong et al., 2019; Li et al., 2019). While these other methods have a similar framework, there has yet to be a comparison between all methods to determine which is most effective. GPIP was selected as it uses the most current classification of regions based on atlases made specifically from fMRI data (Chong et al 2017). Further research should investigate other algorithms for individual parcellation to determine which produces the most accurate individualized parcellation, and whether the results of this study replicate with other algorithms.

BDNF Differences in the Developing Brain

Although this study did not show between group differences of RSFC for Val66Met genotype in healthy young adults, questions remain as to the effects of this SNP in other stages

of life, such as the developing brain. For example, the most robust network differences in RSFC between Val66Met groups were observed by Thomason et al. (2009) in a group of children (mean age = 12); no adult study showed the same level of difference in RSFC within the DMN Executive, or Salience networks. Whereas much of the research on adult populations does not conclusively show RSFC, structural, or behavioural differences in adults, there are studies reliably showing the Val66Met SNP affects all three in children.

Differences in task-related functional connectivity have been identified in children between the left IPL and right SPL for Met carriers relative to Val/Val participants. A study by Jasińska et al. (2016) found lower task activation in Val/Val participants relative to Met carriers when performing language and reading tasks, which has also been associated with worse task performance for the Met carriers relative to Val homozygotes. Findings were distributed, with the IPL being one of the regions showing increased activation. Recently, Mascheretti et al. (2021) followed up on this study, indicating that while they could not find the same effect on reading ability, they did find increased brain activation in reading-related regions for Met carriers 5-13 years old relative to their Val/Val counterparts (2021). Similar to the differences in CT observed between Val/Val and Met carriers, the authors of this study suggest that the differences in activation between genotypes could be the result of the brain compensating for poorer underlying functional connections. This stands in contrast to studies of healthy young adults, which have not consistently identified behavioural differences between Val/Val and Met carriers (Mandelman & Grigorenko, 2012). More studies on behavioural differences, particularly in children, would help to reveal whether there are any group differences in this respect. It also remains to be seen why these differences do not persist into adulthood and are only observed in the developing brain. Further research should be conducted to investigate differences in task-

related functional connectivity in Met carriers with more reading paradigms and at later stages of development to better understand why developmental differences are observed.

As mentioned earlier, CT differences have been observed in Met carrier children relative to Val homozygotes, such that Met carriers had greater CT in lateral occipital, superior parietal and postcentral regions relative to Val/Val participants (de Araujo et al., 2018; Jasińska et al., 2017). Furthermore, other studies have identified hippocampal volume reduction in children who are Met carrier relative to Val/Val (Hashimoto et al., 2016; Toro et al., 2009), whereas many adult studies have not shown this consistently (Gerritsen et al., 2012; Karnik et al., 2010; Koolschijn et al., 2010). This implicates the Met allele in structural developmental differences in the child and adolescent brain. What is not clear, however, is why there would be greater CT for a group where the BDNF protein has a deleterious effect at the cellular level. Furthermore, no explanation has been provided with respect to how these differences in CT are resolved/disappear by young adulthood.

However, it cannot be definitively concluded that the BDNF Val66Met SNP affects brain structure, behaviour, and RSFC of children, as there have been very few studies in this population, unlike studies in adults where a greater number of behavioural and structural studies have been conducted. To date, the study by Thomason et al. is the only study of the effects of the Val66Met SNP on RSFC in children (2009). Meanwhile, structural differences, including reduced hippocampal volume in Met carriers (Hashimoto et al., 2016, Toro et al., 2009) and CT differences across temporal and parietal regions (Jasińska et al., 2017), and behavioural differences in reading ability (Jasińska et al., 2016; Mascheretti et al., 2021) represent the bulk of the limited research on the effect of this SNP in healthy children. Therefore, more studies (both

replication and novel experiments) should be conducted on children to get a better understanding of the Val66Met SNP and differences at the structural, functional, and behavioural levels.

Limitations and Future Directions

The goal of working towards structural and functional connectomes is an important one in our field to gain a better understanding of the interactions between structure and function. However, it is important to consider that said connectomes differ across healthy and diseased populations, as well as between age-groups. For example, studies have identified decreased within network connectivity and greater-between network connectivity in healthy older adults relative to young adults (Chan et al., 2014; Geerligs et al., 2015; Setton et al., 2022; Spreng et al., 2016). Furthermore, in mild cognitive impairment and preclinical Alzheimer's disease, a breakdown in within-network connectivity of the DMN, DAN, and salience networks has been observed (Sheline & Raichle, 2013), and a recent study identified the buildup of amyloid beta and tau proteins in functional hubs of brain networks (Sintini et al., 2021). Therefore, although this study showed no association between the Val66Met SNP and structural/functional differences in the brain, it is important to study this further in disease and across the lifespan. Large neuroimaging datasets like the HCP will assist in these efforts; other HCP researchers are currently working to acquire more varied datasets including diseased, developing, and aging brains, while other projects like the Alzheimer's Disease Neuroimaging Initiative have emerged to study specific diseases and populations (Petersen et al., 2010).

Multivariate methods could prove to be great assets in understanding the extent to which SNP differences like BDNF Val66Met contribute to RSFC. For example, analyses like partial least squares could be used to identify the association between two sets of variables (e.g., brain activity and genotype) by finding spatiotemporal patterns of covariance that most optimally

differentiate the variables. This data-driven approach, which could consider the relationship between multiple independent variables, could provide insight into the relationship between the Val66Met SNP and RSFC that would not be possible in univariate analyses. A study by Setton et al. (2022), who used multivariate methods to study the differences in RSFC and network differentiation between younger and older adults, provides a good framework for future studies aiming to perform a rigorous, data-driven study of genotypes and intrinsic functional networks.

This thesis used the FreeSurfer cortical surface reconstruction measures of CT in all analyses involving CT. Importantly, these measures are an estimation of CT based on the reconstruction of the white matter and pial matter surfaces; they do not represent a direct measurement of CT (although a direct measurement would not be possible without invasive methods). As such, the measures of CT could vary if a different processing approach were used (for example, the Computational Anatomy Toolbox being used to calculate CT instead of FreeSurfer), as different methods of calculating CT are taken (Seiger et al., 2018). This limitation is not a cause for concern, as cortical parcellations and CT measures taken from FreeSurfer are widely utilized and considered one of the most reliable approaches to measuring CT (Dale et al., 1999; Fischl & Dale, 2000; Seiger et al., 2018). Nevertheless, it may be worthwhile to replicate CT analyses with an alternative approach to verify the findings of no significant differences between Val66Met genotype in CT.

Another limitation stems from the fact that the RSFC data available for this study comprised only Fisher-Z scores for every pairwise correlation among the 400 parcels (GPIP transformed) of the Schaefer atlas (Schaefer et al., 2018). Additional data, such as the GPIP output files delineating the individually parcellated brain regions for all participants, would have been useful to further validate the accuracy of functional parcellation for every participant and

the RSFC correlation values between each pairwise ROI. Moreover, it would have allowed for analyses of functional parcels at different levels of spatial resolution (e.g., 200 vs. 400 parcels). In the future, my analyses should be replicated with both HCP participants and other samples of healthy young adults, following the GPIP processing steps, to determine if any of the additional data can provide further insights into the relationship between the Val66Met SNP and RSFC in healthy young adults.

The Val66Met SNP has been linked to the effectiveness of transcranial magnetic stimulation in healthy young adults, most notably with intermittent and continuous theta burst stimulation (iTBS and cTBS, respectively). Previous studies have demonstrated that Val/Val participants show increased cortical excitability after iTBS and reduced excitability after cTBS at the motor cortex, while Met carriers show no significant change in motor evoked potential following stimulation with either iTBS (Antal et al., 2010; Cheeran et al., 2008) or cTBS (Cheeran et al., 2008). In a previous case study of two participants, one Val/Val and the other Met/Met, I observed that the Met/Met participant did not respond as strongly as the Val/Val participant to iTBS and cTBS when attempting to modulate RSFC of the DMN (Alba Suarez, 2020). These studies point to a possible interaction between the Val66Met SNP and transcranial magnetic stimulation, which could impact applications of TBS in treating major depressive disorder (George et al., 2000) and enhancing cognitive performance (Walsh et al., 1998). Researchers should continue to explore the potential effects that this BDNF polymorphism may have on iTBS, cTBS, and other transcranial magnetic stimulation protocols to better understand whether these non-invasive stimulation approaches have genotype-dependent viability.

A limitation affecting both the structural and functional analyses in the current study was the limited sample sizes of Val/Met and Met/Met groups. While this is to be expected, given the

low gene frequency in the North American population studied (Petryshen et al., 2010), researchers in North America will always face difficulties in recruiting adequate numbers of participants with the Met allele. While a larger sample of Met carriers could be recruited from different regions with higher frequencies of this SNP (e.g., Asia), there is research to suggest that the Met allele has different effects across different ethnicities. For example, researchers have identified differences in the effectiveness of antidepressants between Asian and Caucasian samples, where Asian Met allele carriers have a better response (e.g., better efficacy) to SSRIs relative to their Caucasian counterparts (Yan et al., 2014). An important next step, then, is to find a way to recruit a larger sample of Val/Met and Met/Met participants to increase statistical power in future research. Alternatively, a dataset with a larger number of participants, such as the UK Biobank, could be used in future studies to acquire a more diverse (albeit older) sample that is likely to have many more Met/Met participants.

Conclusion

The Val66Met SNP of BDNF has been implicated as a factor affecting structural integrity at the level of CT, and functional differences as measured by RSFC. However, previous studies have been limited both by sample size and the methods available at the time. Using cutting-edge methods and a larger sample of participants from the HCP project, I set out to determine whether the Val66Met SNP has any effect on structural or functional network integrity in healthy young adult participants by measuring CT and RSFC within and between networks. No significant differences were identified in CT measures between genotype groups (with one exception which was later found to have significant outliers leading to this result). No significant differences in RSFC were found between the genotype comparisons in within-network or between-network RSFC. Altogether, these findings suggest that the Val66Met SNP does not moderate structural or

functional differences in healthy young adults. These results highlight the importance of using individualized functional parcellations in studies of intrinsic functional brain networks, studying different age groups/developmental stages of the brain in neurosciences, and using large samples of participants such as the HCP in genetic analyses. Future studies should further investigate Val66Met genotype differences in structure and function observed in the developing brain, as well as other populations, including diseased and older adults, to get a better understanding of the effects of this SNPs across the lifespan.

References

Alba Suarez, V. (2020). *Influence of the Brain Derived Neurotrophic Factor Val66Met Polymorphism on the Modulation of Functional Brain Networks through Thetaburst Transcranial Magnetic Stimulation*. York University.

Andreasen, N. C., O'Leary, D. S., Cizadlo, T., Arndt, S., Rezai, K., Watkins, G. L., Boles Ponto, L. L., & Hichwa, R. D. (1995). Remembering the past: Two facets of episodic memory explored with positron emission tomography. *American Journal of Psychiatry*, *152*(11), 1576–1585. https://doi.org/10.1176/ajp.152.11.1576

Andrews-Hanna, J. R., Reidler, J. S., Sepulcre, J., Poulin, R., & Buckner, R. L. (2010). Functional-Anatomic Fractionation of the Brain's Default Network. *Neuron*, *65*(4), 550–562. https://doi.org/10.1016/j.neuron.2010.02.005

Andrews-Hanna, J. R., Smallwood, J., & Spreng, R. N. (2014). The default network and self-generated thought: component processes, dynamic control, and clinical relevance. *Annals of the New York Academy of Sciences*, *1316*(1), 29. https://doi.org/10.1111/NYAS.12360

Antal, A., Chaieb, L., Moliadze, V., Monte-Silva, K., Poreisz, C., Thirugnanasambandam, N., Nitsche, M. A., Shoukier, M., Ludwig, H., & Paulus, W. (2010). Brain-derived neurotrophic factor (BDNF) gene polymorphisms shape cortical plasticity in humans. *Brain Stimulation*, *3*(4), 230–237. https://doi.org/10.1016/j.brs.2009.12.003

Barde, Y. A., Edgar, D., & Thoenen, H. (1982). Purification of a new neurotrophic factor from mammalian brain. *Hoppe-Seyler's Zeitschrift Fur Physiologische Chemie*, *363*(11), 1295–1296. https://doi.org/10.1002/j.1460-2075.1982.tb01207.x

Bathina, S., & Das, U. N. (2015). Brain-derived neurotrophic factor and its clinical Implications.

In *Archives of Medical Science* (Vol. 11, Issue 6, pp. 1164–1178). Termedia Publishing House Ltd. https://doi.org/10.5114/aoms.2015.56342

Bekinschtein, P., Cammarota, M., Katche, C., Slipczuk, L., Rossato, J. I., Goldin, A., Izquierdo, I., & Medina, J. H. (2008). BDNF is essential to promote persistence of long-term memory storage. *Proceedings of the National Academy of Sciences of the United States of America*, *105*(7), 2711–2716. https://doi.org/10.1073/pnas.0711863105

Benjamini, Y., & Hochberg, Y. (1995). Controlling the False Discovery Rate: A Practical and Powerful Approach to Multiple Testing. *Journal of the Royal Statistical Society. Series B (Methodological)*, *57*(1), 289–300.

Beste, C., Schneider, D., Epplen, J. T., & Arning, L. (2011). The functional BDNF Val66Met polymorphism affects functions of pre-attentive visual sensory memory processes. *Neuropharmacology*, *60*(2–3), 467–471. https://doi.org/10.1016/j.neuropharm.2010.10.028

Biswal, B., Zerrin Yetkin, F., Haughton, V. M., & Hyde, J. S. (1995). Functional connectivity in the motor cortex of resting human brain using echo-planar mri. *Magnetic Resonance in Medicine*, *34*(4), 537–541. https://doi.org/10.1002/mrm.1910340409

Blumensath, T., Jbabdi, S., Glasser, M. F., Van Essen, D. C., Ugurbil, K., Behrens, T. E. J., & Smith, S. M. (2013). Spatially constrained hierarchical parcellation of the brain with resting-state fMRI. *NeuroImage*, *76*, 313. https://doi.org/10.1016/J.NEUROIMAGE.2013.03.024

Brunet, A., Bonni, A., Zigmond, M. J., Lin, M. Z., Juo, P., Hu, L. S., Anderson, M. J., Arden, K. C., Blenis, J., & Greenberg, M. E. (1999). Akt promotes cell survival by phosphorylating and inhibiting a forkhead transcription factor. *Cell*, *96*(6), 857–868.

https://doi.org/10.1016/S0092-8674(00)80595-4

Buckner, R. L., Andrews-Hanna, J. R., & Schacter, D. L. (2008). The brain's default network: Anatomy, function, and relevance to disease. *Annals of the New York Academy of Sciences*, *1124*, 1–38. https://doi.org/10.1196/annals.1440.011

Bueller, J. A., Aftab, M., Sen, S., Gomez-Hassan, D., Burmeister, M., & Zubieta, J. K. (2006). BDNF Val66Met Allele Is Associated with Reduced Hippocampal Volume in Healthy Subjects. *Biological Psychiatry*, *59*(9), 812–815. https://doi.org/10.1016/J.BIOPSYCH.2005.09.022

Carballedo, A., Amico, F., Ugwu, I., Fagan, A. J., Fahey, C., Morris, D., Meaney, J. F., Leemans, A., & Frodl, T. (2012). Reduced fractional anisotropy in the uncinate fasciculus in patients with major depression carrying the met-allele of the Val66Met brain-derived neurotrophic factor genotype. *American Journal of Medical Genetics Part B: Neuropsychiatric Genetics*, *159B*(5), 537–548. https://doi.org/10.1002/AJMG.B.32060

Carmelli, D., DeCarli, C., Swan, G. E., Jack, L. M., Reed, T., Wolf, P. A., & Miller, B. L. (1998). Evidence For Genetic Variance in White Matter Hyperintensity Volume in Normal Elderly Male Twins. *Stroke*, *29*(6), 1177–1181. https://doi.org/10.1161/01.STR.29.6.1177

Chan, M. Y., Park, D. C., Savalia, N. K., Petersen, S. E., & Wig, G. S. (2014). Decreased segregation of brain systems across the healthy adult lifespan. *Proceedings of the National Academy of Sciences of the United States of America*, *111*(46), E4997–E5006. https://doi.org/10.1073/PNAS.1415122111/SUPPL_FILE/PNAS.1415122111.SAPP.PDF

Cheeran, B., Talelli, P., Mori, F., Koch, G., Suppa, A., Edwards, M., Houlden, H., Bhatia, K., Greenwood, R., & Rothwell, J. C. (2008). A common polymorphism in the brain-derived

neurotrophic factor gene (BDNF) modulates human cortical plasticity and the response to rTMS. *Journal of Physiology*, *586*(23), 5717–5725. https://doi.org/10.1113/jphysiol.2008.159905

Chen, Z. Y., Jing, D., Bath, K. G., Ieraci, A., Khan, T., Siao, C. J., Herrera, D. G., Toth, M., Yang, C., McEwen, B. S., Hempstead, B. L., & Lee, F. S. (2006). Genetic variant BDNF (Val66Met) polymorphism alters anxiety-related behavior. *Science*, *314*(5796), 140–143. https://doi.org/10.1126/science.1129663

Chen, Z. Y., Patel, P. D., Sant, G., Meng, C. X., Teng, K. K., Hempstead, B. L., & Lee, F. S. (2004). Variant Brain-Derived Neurotrophic Factor (BDNF) (Met66) Alters the Intracellular Trafficking and Activity-Dependent Secretion of Wild-Type BDNF in Neurosecretory Cells and Cortical Neurons. *Journal of Neuroscience*, *24*(18), 4401–4411. https://doi.org/10.1523/JNEUROSCI.0348-04.2004

Chepenik, L. G., Fredericks, C., Papademetris, X., Spencer, L., Lacadie, C., Wang, F., Pittman, B., Duncan, J. S., Staib, L. H., Duman, R. S., Gelernter, J., & Blumberg, H. P. (2009). Effects of the Brain-Derived Neurotrophic Growth Factor Val66Met Variation on Hippocampus Morphology in Bipolar Disorder. *Neuropsychopharmacology*, *34*(4), 944–951. https://doi.org/10.1038/npp.2008.107

Chong, M., Bhushan, C., Joshi, A. A., Choi, S., Haldar, J. P., Shattuck, D. W., Spreng, R. N., & Leahy, R. M. (2017). Individual parcellation of resting fMRI with a group functional connectivity prior. *NeuroImage*, *156*(May), 87–100. https://doi.org/10.1016/j.neuroimage.2017.04.054

Cieri, F., Zhuang, X., Cordes, D., Kaplan, N., Cummings, J., & Caldwell, J. (2022). Relationship

of sex differences in cortical thickness and memory among cognitively healthy subjects and individuals with mild cognitive impairment and Alzheimer disease. *Alzheimer's Research and Therapy*, *14*(1), 1–12. https://doi.org/10.1186/S13195-022-00973-1/FIGURES/4

Cole, D. M., Smith, S. M., & Beckmann, C. F. (2010). Advances and pitfalls in the analysis and interpretation of resting-state FMRI data. *Frontiers in Systems Neuroscience*, *4*, 8. https://doi.org/10.3389/FNSYS.2010.00008/BIBTEX

Corbetta, M., & Shulman, G. L. (2002). Control of goal-directed and stimulus-driven attention in the brain. *Nature Reviews Neuroscience*, *3*(3), 201–215. https://doi.org/10.1038/nrn755

Dale, A. M., Fischl, B., & Sereno, M. I. (1999). Cortical Surface-Based Analysis: I. Segmentation and Surface Reconstruction. *NeuroImage*, *9*(2), 179–194. https://doi.org/10.1006/NIMG.1998.0395

de Araujo, C. M., Zugman, A., Swardfager, W., Belangero, S. I. N., Ota, V. K., Spindola, L. M., Hakonarson, H., Pellegrino, R., Gadelha, A., Salum, G. A., Pan, P. M., de Moura, L. M., Del Aquilla, M., Picon, F. A., Amaro, E., Sato, J. R., Brietzke, E., Grassi-Oliveira, R., Rohde, L. A. P., … Jackowski, A. P. (2018). Effects of the brain-derived neurotropic factor variant Val66Met on cortical structure in late childhood and early adolescence. *Journal of Psychiatric Research*, *98*(December 2017), 51–58. https://doi.org/10.1016/j.jpsychires.2017.12.008

Dempster, E., Toulopoulou, T., McDonald, C., Bramon, E., Walshe, M., Filbey, F., Wickham, H., Sham, P. C., Murray, R. M., & Collier, D. A. (2005). Association between BDNF val66 met genotype and episodic memory. *American Journal of Medical Genetics - Neuropsychiatric Genetics*, *134 B*(1), 73–75. https://doi.org/10.1002/ajmg.b.30150

Desikan, R. S., Ségonne, F., Fischl, B., Quinn, B. T., Dickerson, B. C., Blacker, D., Buckner, R. L., Dale, A. M., Maguire, R. P., Hyman, B. T., Albert, M. S., & Killiany, R. J. (2006). An automated labeling system for subdividing the human cerebral cortex on MRI scans into gyral based regions of interest. *NeuroImage*, *31*(3), 968–980. https://doi.org/10.1016/j.neuroimage.2006.01.021

Du, Y., Fischer, T. Z., Lee, L. N., Lercher, L. D., & Dreyfus, C. F. (2003). Regionally Specific Effects of BDNF on Oligodendrocytes. *Dev Neurosci*, *25*, 116–126. https://doi.org/10.1159/000072261

Duman, R. S., & Monteggia, L. M. (2006). A Neurotrophic Model for Stress-Related Mood Disorders. *Biological Psychiatry*, *59*(12), 1116–1127. https://doi.org/10.1016/j.biopsych.2006.02.013

Egan, M. F., Kojima, M., Callicott, J. H., Goldberg, T. E., Kolachana, B. S., Bertolino, A., Zaitsev, E., Gold, B., Goldman, D., Dean, M., Lu, B., & Weinberger, D. R. (2003). The BDNF val66met polymorphism affects activity-dependent secretion of BDNF and human memory and hippocampal function. *Cell*, *112*(2), 257–269. https://doi.org/10.1016/S0092-8674(03)00035-7

Ekman, M., Derrfuss, J., Tittgemeyer, M., & Fiebach, C. J. (2012). Predicting errors from reconfiguration patterns in human brain networks. *Proceedings of the National Academy of Sciences of the United States of America*, *109*(41), 16714–16719. https://doi.org/10.1073/pnas.1207523109

Fischl, B., & Dale, A. M. (2000). Measuring the thickness of the human cerebral cortex from magnetic resonance images. *Proceedings of the National Academy of Sciences*, *97*(20),

11050–11055. https://doi.org/10.1073/PNAS.200033797

Fletcher, J. L., Murray, S. S., & Xiao, J. (2018). Brain-derived neurotrophic factor in central nervous system myelination: A new mechanism to promote myelin plasticity and repair. *International Journal of Molecular Sciences*, *19*(12). https://doi.org/10.3390/IJMS19124131

Fox, M. D., & Greicius, M. (2010). Clinical applications of resting state functional connectivity. *Frontiers in Systems Neuroscience*, *4*, 19. https://doi.org/10.3389/FNSYS.2010.00019/BIBTEX

Fox, M. D., Snyder, A. Z., Vincent, J. L., Corbetta, M., Van Essen, D. C., & Raichle, M. E. (2005). The human brain is intrinsically organized into dynamic, anticorrelated functional networks. *Proceedings of the National Academy of Sciences of the United States of America*, *102*(27), 9673–9678. https://doi.org/10.1073/pnas.0504136102

Friston, K. J., Williams, S., Howard, R., Frackowiak, R. S. J., & Turner, R. (1996). Movement-Related effects in fMRI time-series. *Magnetic Resonance in Medicine*, *35*(3), 346–355. https://doi.org/10.1002/MRM.1910350312

Geerligs, L., Renken, R. J., Saliasi, E., Maurits, N. M., & Lorist, M. M. (2015). A Brain-Wide Study of Age-Related Changes in Functional Connectivity. *Cerebral Cortex*, *25*(7), 1987–1999. https://doi.org/10.1093/cercor/bhu012

George, M. S., Nahas, Z., Molloy, M., Speer, A. M., Oliver, N. C., Li, X. B., Arana, G. W., Risch, S. C., & Ballenger, J. C. (2000). A controlled trial of daily left prefrontal cortex TMS for treating depression. *Biological Psychiatry*, *48*(10), 962–970. https://doi.org/10.1016/S0006-3223(00)01048-9

Gerritsen, L., Tendolkar, I., Franke, B., Vasquez, A. A., Kooijman, S., Buitelaar, J., Fernández, G., & Rijpkema, M. (2012). BDNF Val66Met genotype modulates the effect of childhood adversity on subgenual anterior cingulate cortex volume in healthy subjects. *Molecular Psychiatry*, *17*(6), 597–603. https://doi.org/10.1038/mp.2011.51

Gholipour, A., Kehtarnavaz, N., Briggs, R., Devous, M., & Gopinath, K. (2007). Brain Functional Localization: A Survey of Image Registration Techniques. *IEEE Transactions on Medical Imaging*, *26*(4), 427–451. https://doi.org/10.1109/TMI.2007.892508

Glasser, M. F., Sotiropoulos, S. N., Wilson, J. A., Coalson, T. S., Fischl, B., Andersson, J. L., Xu, J., Jbabdi, S., Webster, M., Polimeni, J. R., Van Essen, D. C., & Jenkinson, M. (2013). The Minimal Preprocessing Pipelines for the Human Connectome Project and for the WU-Minn HCP Consortium. *Neuroimage*, *80*, 105–12404. https://doi.org/10.1016/j.neuroimage.2013.04.127.The

Glezer, L. S., & Riesenhuber, M. (2013). Individual Variability in Location Impacts Orthographic Selectivity in the "Visual Word Form Area." *Journal of Neuroscience*, *33*(27), 11221–11226. https://doi.org/10.1523/JNEUROSCI.5002-12.2013

Gordon, E. M., Laumann, T. O., Adeyemo, B., & Petersen, S. E. (2015). Individual Variability of the System-Level Organization of the Human Brain. *Cerebral Cortex*, *27*(1), bhv239. https://doi.org/10.1093/cercor/bhv239

Hall, D., Dhilla, A., Charalambous, A., Gogos, J. A., & Karayiorgou, M. (2003). Sequence variants of the brain-derived neurotrophic factor (BDNF) gene are strongly associated with obsessive-compulsive disorder. *American Journal of Human Genetics*, *73*(2), 370–376. https://doi.org/10.1086/377003

Hansen, B. B. (2004). Full Matching in an Observational Study of Coaching for the SAT. *Journal of the American Statistical Association*, *99*(467), 609–618. https://doi.org/10.1198/016214504000000647

Hashimoto, T., Fukui, K., Takeuchi, H., Yokota, S., Kikuchi, Y., Tomita, H., Taki, Y., & Kawashima, R. (2016). Effects of the BDNF Val66Met Polymorphism on Gray Matter Volume in Typically Developing Children and Adolescents. *Cerebral Cortex (New York, NY)*, *26*(4), 1795. https://doi.org/10.1093/CERCOR/BHW020

He, Y., Chen, Z. J., & Evans, A. C. (2007). Small-World Anatomical Networks in the Human Brain Revealed by Cortical Thickness from MRI. *Cerebral Cortex*, *17*(10), 2407–2419. https://doi.org/10.1093/CERCOR/BHL149

Hermundstad, A. M., Bassett, D. S., Brown, K. S., Aminoff, E. M., Clewett, D., Freeman, S., Frithsen, A., Johnson, A., Tipper, C. M., Miller, M. B., Grafton, S. T., & Carlson, J. M. (2013). Structural foundations of resting-state and task-based functional connectivity in the human brain. *Proceedings of the National Academy of Sciences of the United States of America*, *110*(15), 6169–6174. https://doi.org/10.1073/PNAS.1219562110/SUPPL_FILE/SAPP.PDF

Ho, B.-C., Milev, P., O'Leary, D. S., Librant, A., Andreasen, N. C., & Wassink, T. H. (2006). Cognitive and Magnetic Resonance Imaging Brain Morphometric Correlates of Brain-Derived Neurotrophic Factor Val66Met Gene Polymorphism in Patients With Schizophrenia and Healthy Volunteers. *Archives of General Psychiatry*, *63*(7), 731. https://doi.org/10.1001/archpsyc.63.7.731

Ho, D. E., Imai, K., King, G., & Stuart, E. A. (2011). MatchIt: Nonparametric Preprocessing for

Parametric Causal Inference. *Journal of Statistical Software*, *42*(8), 1–28. https://doi.org/10.18637/JSS.V042.I08

Ho, D. E., Imai, K., King, G., Stuart, E. A., Abadie, A., Beck, N., Cook, S., Diamond, A., Hansen, B., Imbens, G., Lau, O., Lenz, G., Rosenbaum, P., & Rubin, D. (2007). Matching as Nonparametric Preprocessing for Reducing Model Dependence in Parametric Causal Inference. *Political Analysis*, *15*, 199–236. https://doi.org/10.1093/pan/mpl013

Honey, C. J., Sporns, O., Cammoun, L., Gigandet, X., Thiran, J. P., Meuli, R., & Hagmann, P. (2009). Predicting human resting-state functional connectivity from structural connectivity. *Proceedings of the National Academy of Sciences of the United States of America*, *106*(6), 2035. https://doi.org/10.1073/PNAS.0811168106

Hosang, G. M., Shiles, C., Tansey, K. E., McGuffin, P., & Uher, R. (2014). Interaction between stress and the BDNFVal66Met polymorphism in depression: a systematic review and meta-analysis. *BMC Medicine*, *12*(1), 7. https://doi.org/10.1186/1741-7015-12-7

IBM Corp. (2021). *IBM SPSS Statistics for Windows, Version 28.0*.

Jackson, M., Marks, L., May, G. H. W., & Wilson, J. B. (2018). The genetic basis of disease. *Essays in Biochemistry*, *62*(5), 643. https://doi.org/10.1042/EBC20170053

Jang, J. H., Yun, J. Y., Jung, W. H., Shim, G., Byun, M. S., Hwang, J. Y., Kim, S. N., Choi, C. H., & Kwon, J. S. (2012). The impact of genetic variation in COMT and BDNF on resting-state functional connectivity. *International Journal of Imaging Systems and Technology*, *22*(1), 97–102. https://doi.org/10.1002/ima.22000

Jasińska, K. K., Molfese, P. J., Kornilov, S. A., Mencl, W. E., Frost, S. J., & Lee, M. (2016). The

BDNF Val 66 Met Polymorphism Influences Reading Ability and Patterns of Neural Activation in Children. *PLoS ONE*, *11*(8), 157449. https://doi.org/10.1371/journal.pone.0157449

Jasínska, K. K., Molfese, P. J., Kornilov, S. A., Mencl, W. E., Frost, S. J., Lee, M., Pugh, K. R., Grigorenko, E. L., & Landi, N. (2017). The BDNF Val 66 Met polymorphism is associated with structural neuroanatomical differences in young children. *Behavioural Brain Research*, *328*, 48–56. https://doi.org/10.1016/j.bbr.2017.03.014

Johnson, J. E., Barde, Y. A., Schwab, M., & Thoenen, H. (1986). Brain-derived neurotrophic factor supports the survival of cultured rat retinal ganglion cells. *Journal of Neuroscience*, *6*(10), 3031–3038. https://doi.org/10.1523/jneurosci.06-10-03031.1986

Karnik, M. S., Wang, L., Barch, D. M., Morris, J. C., & Csernansky, J. G. (2010). BDNF polymorphism rs6265 and hippocampal structure and memory performance in healthy control subjects. *Psychiatry Research*, *178*(2), 425. https://doi.org/10.1016/J.PSYCHRES.2009.09.008

Kerepesi, C., Szalkai, B., Varga, B., & Grolmusz, V. (2018). Comparative connectomics: Mapping the inter-individual variability of connections within the regions of the human brain. *Neuroscience Letters*, *662*, 17–21. https://doi.org/10.1016/j.neulet.2017.10.003

Khalili-Mahani, N., Zoethout, R. M. W., Beckmann, C. F., Baerends, E., de Kam, M. L., Soeter, R. P., Dahan, A., van Buchem, M. A., van Gerven, J. M. A., & Rombouts, S. A. R. B. (2012). Effects of morphine and alcohol on functional brain connectivity during "resting state":A placebo-controlled crossover study in healthy young men. *Human Brain Mapping*, *33*(5), 1003–1018. https://doi.org/10.1002/hbm.21265

Klein, R., Nanduri, V., Jing, S., Lamballe, F., Tapley, P., Bryant, S., Cordon-Cardo, C., Jones, K. R., Reichardt, L. F., & Barbacid, M. (1991). The trkB tyrosine protein kinase is a receptor for brain-derived neurotrophic factor and neurotrophin-3. *Cell*, *66*(2), 395–403. https://doi.org/10.1016/0092-8674(91)90628-C

Knecht, S., Dräger, B., Deppe, M., Bobe, L., Lohmann, H., Flöel, A., Ringelstein, E. B., & Henningsen, H. (2000). Handedness and hemispheric language dominance in healthy humans. *Brain*, *123*(12), 2512–2518. https://doi.org/10.1093/BRAIN/123.12.2512

Kong, R., Li, J., Orban, C., Sabuncu, M. R., Liu, H., Schaefer, A., Sun, N., Zuo, X. N., Holmes, A. J., Eickhoff, S. B., & Yeo, B. T. T. (2019). Spatial Topography of Individual-Specific Cortical Networks Predicts Human Cognition, Personality, and Emotion. *Cerebral Cortex*, *29*(6), 2533–2551. https://doi.org/10.1093/CERCOR/BHY123

Koolschijn, P. C. M. P., Van Haren, N. E. M., Bakker, S. C., Hoogendoorn, M. L. C., Hulshoff Pol, H. E., & Kahn, R. S. (2010). Effects of brain-derived neurotrophic factor Val66Met polymorphism on hippocampal volume change in schizophrenia. *Hippocampus*, *20*(9), 1010–1017. https://doi.org/10.1002/HIPO.20699

Lerch, J. P., Worsley, K., Shaw, W. P., Greenstein, D. K., Lenroot, R. K., Giedd, J., & Evans, A. C. (2006). Mapping anatomical correlations across cerebral cortex (MACACC) using cortical thickness from MRI. *NeuroImage*, *31*(3), 993–1003. https://doi.org/10.1016/j.neuroimage.2006.01.042

Levine, E. S., Crozier, R. A., Black, I. B., & Plummer, M. R. (1998). Brain-derived neurotrophic factor modulates hippocampal synaptic transmission by increasing N-methyl-D-aspartic acid receptor activity. *Proceedings of the National Academy of Sciences of the United States*

of America, *95*(17), 10235–10239. https://doi.org/10.1073/pnas.95.17.10235

Li, M., Wang, D., Ren, J., Langs, G., Stoecklein, S., Brennan, B. P., Lu, J., Chen, H., & Liu, H. (2019). Performing group-level functional image analyses based on homologous functional regions mapped in individuals. *PLOS Biology*, *17*(3), e2007032. https://doi.org/10.1371/JOURNAL.PBIO.2007032

Lim, Y. Y., Hassenstab, J., Cruchaga, C., Goate, A., Fagan, A. M., Benzinger, T. L. S., Maruff, P., Snyder, P. J., Masters, C. L., Allegri, R., Chhatwal, J., Farlow, M. R., Graff-Radford, N. R., Laske, C., Levin, J., McDade, E., Ringman, J. M., Rossor, M., Salloway, S., … Bateman, R. J. (2016). BDNF Val66Met moderates memory impairment, hippocampal function and tau in preclinical autosomal dominant Alzheimer's disease. *Brain*, *139*(10), 2766–2777. https://doi.org/10.1093/brain/aww200

Lim, Y. Y., Laws, S. M., Perin, S., Pietrzak, R. H., Fowler, C., Masters, C. L., & Maruff, P. (2021). BDNF VAL66MET polymorphism and memory decline across the spectrum of Alzheimer's disease. *Genes, Brain and Behavior*, *20*(5), 1–9. https://doi.org/10.1111/gbb.12724

Mailman, M. D., Feolo, M., Jin, Y., Kimura, M., Tryka, K., Bagoutdinov, R., Hao, L., Kiang, A., Paschall, J., Phan, L., Popova, N., Pretel, S., Ziyabari, L., Lee, M., Shao, Y., Wang, Z. Y., Sirotkin, K., Ward, M., Kholodov, M., … Sherry, S. T. (2007). The NCBI dbGaP database of genotypes and phenotypes. *Nature Genetics*, *39*(10), 1181. https://doi.org/10.1038/NG1007-1181

Mandelman, S. D., & Grigorenko, E. L. (2012). BDNF Val66Met and cognition: all, none, or some? A meta-analysis of the genetic association. *Genes, Brain and Behavior*, *11*(2), 127–

136. https://doi.org/10.1111/j.1601-183X.2011.00738.x

Marcus, D. S., Harwell, J., Olsen, T., Hodge, M., Glasser, M. F., Prior, F., Jenkinson, M., Laumann, T., Curtiss, S. W., & Van Essen, D. C. (2011). Informatics and data mining tools and strategies for the human connectome project. *Frontiers in Neuroinformatics*, *5*, 4. https://doi.org/10.3389/FNINF.2011.00004/XML/NLM

Mascheretti, S., Perdue, M. V, Feng, B., Andreola, C., Dionne, G., Jasińska, K. K., Pugh, K. R., Grigorenko, E. L., & Landi, N. (2021). From BDNF to reading: Neural activation and phonological processing as multiple mediators. *Behavioural Brain Research*, *396*, 112859. https://doi.org/10.1016/j.bbr.2020.112859

Mathworks Inc. (2019). *MATLAB and Statistics Toolbox Release 2019b*. The Mathworks Inc.

McCulloch, D. E. W., Madsen, M. K., Stenbæk, D. S., Kristiansen, S., Ozenne, B., Jensen, P. S., Knudsen, G. M., & Fisher, P. M. D. (2022). Lasting effects of a single psilocybin dose on resting-state functional connectivity in healthy individuals. *Journal of Psychopharmacology*, *36*(1), 74–84. https://doi.org/10.1177/02698811211026454

McIntosh, A. R. (2000). Towards a network theory of cognition. *Neural Networks : The Official Journal of the International Neural Network Society*, *13*(8–9), 861–870. https://doi.org/10.1016/S0893-6080(00)00059-9

Miyajima, F., Ollier, W., Mayes, A., Jackson, A., Thacker, N., Rabbitt, P., Pendleton, N., Horan, M., & Payton, A. (2008). Brain-derived neurotrophic factor polymorphism Val66Met influences cognitive abilities in the elderly. *Genes, Brain and Behavior*, *7*(4), 411–417. https://doi.org/10.1111/j.1601-183X.2007.00363.x

Mizui, T., Ishikawa, Y., Kumanogoh, H., Lume, M., Matsumoto, T., Hara, T., Yamawaki, S., Takahashi, M., Shiosaka, S., Itami, C., Uegaki, K., Saarma, M., & Kojima, M. (2015). BDNF pro-peptide actions facilitate hippocampal LTD and are altered by the common BDNF polymorphism Val66Met. *Proceedings of the National Academy of Sciences of the United States of America*, *112*(23), E3067–E3074. https://doi.org/10.1073/PNAS.1422336112/-/DCSUPPLEMENTAL

Molendijk, M. L., Bus, B. A. A., Spinhoven, P., Kaimatzoglou, A., Voshaar, R. C. O., Penninx, B. W. J. H., van Ijzendoorn, M. H., & Elzinga, B. M. (2012). A systematic review and meta-analysis on the association between BDNF val66met and hippocampal volume—A genuine effect or a winners curse? *American Journal of Medical Genetics Part B: Neuropsychiatric Genetics*, *159B*(6), 731–740. https://doi.org/10.1002/AJMG.B.32078

Mueller, S., Wang, D., Fox, M. D., Yeo, B. T. T., Sepulcre, J., Sabuncu, M. R., Shafee, R., Lu, J., & Liu, H. (2013). Individual Variability in Functional Connectivity Architecture of the Human Brain. *Neuron*, *77*(3), 586. https://doi.org/10.1016/J.NEURON.2012.12.028

Müller, F., Holze, F., Dolder, P., Ley, L., Vizeli, P., Soltermann, A., Liechti, M. E., & Borgwardt, S. (2021). MDMA-induced changes in within-network connectivity contradict the specificity of these alterations for the effects of serotonergic hallucinogens. *Neuropsychopharmacology*, *46*(3), 545–553. https://doi.org/10.1038/s41386-020-00906-2

Ogawa, S., Lee, T. -M, Nayak, A. S., & Glynn, P. (1990). Oxygenation-sensitive contrast in magnetic resonance image of rodent brain at high magnetic fields. *Magnetic Resonance in Medicine*, *14*(1), 68–78. https://doi.org/10.1002/mrm.1910140108

Oldfield, R. C. (1971). The assessment and analysis of handedness: The Edinburgh inventory.

Neuropsychologia, *9*(1), 97–113. https://doi.org/10.1016/0028-3932(71)90067-4

Park, C., Kim, J., Namgung, E., Lee, D. W., Kim, G. H., Kim, M., Kim, N., Kim, T. D., Kim, S., Lyoo, I. K., & Yoon, S. (2017). The BDNF val66met polymorphism affects the vulnerability of the brain structural network. *Frontiers in Human Neuroscience*, *11*(August), 1–10. https://doi.org/10.3389/fnhum.2017.00400

Park, H.-J., & Friston, K. (2013). Structural and functional brain networks: From connections to cognition. *Science*, *342*(6158). https://doi.org/10.1126/SCIENCE.1238411

Patterson, S. L., Abel, T., Deuel, T. A. S., Martin, K. C., Rose, J. C., & Kandel, E. R. (1996). Recombinant BDNF rescues deficits in basal synaptic transmission and hippocampal LTP in BDNF knockout mice. *Neuron*, *16*(6), 1137–1145. https://doi.org/10.1016/S0896-6273(00)80140-3

Petersen, R. C., Aisen, P. S., Beckett, L. A., Donohue, M. C., Gamst, A. C., Harvey, D. J., Jack, C. R., Jagust, W. J., Shaw, L. M., Toga, A. W., Trojanowski, J. Q., & Weiner, M. W. (2010). Alzheimer's Disease Neuroimaging Initiative (ADNI): Clinical characterization. *Neurology*, *74*(3), 201–209. https://doi.org/10.1212/WNL.0b013e3181cb3e25

Petryshen, T. L., Sabeti, P. C., Aldinger, K. A., Fry, B., Fan, J. B., Schaffner, S. F., Waggoner, S. G., Tahl, A. R., & Sklar, P. (2010). Population genetic study of the brain-derived neurotrophic factor (BDNF) gene. *Molecular Psychiatry*, *15*(8), 810–815. https://doi.org/10.1038/mp.2009.24

Pezawas, L., Verchinski, B. A., Mattay, V. S., Callicott, J. H., Kolachana, B. S., Straub, R. E., Egan, M. F., Meyer-Lindenberg, A., & Weinberger, D. R. (2004). The brain-derived neurotrophic factor val66met polymorphism and variation in human cortical morphology.

Journal of Neuroscience, *24*(45), 10099–10102. https://doi.org/10.1523/JNEUROSCI.2680-04.2004

Querbes, O., Aubry, F., Pariente, J., Lotterie, J. A., Dmonet, J. F., Duret, V., Puel, M., Berry, I., Fort, J. C., & Celsis, P. (2009). Early diagnosis of Alzheimer's disease using cortical thickness: impact of cognitive reserve. *Brain*, *132*(8), 2036–2047. https://doi.org/10.1093/BRAIN/AWP105

R Core Team. (2022). *R: A language and environment for statistical computing*. R Foundation for Statistical Computing, Vienna, Austria.

Ribasés, M., Gratacòs, M., Fernández-Aranda, F., Bellodi, L., Boni, C., Anderluh, M., Cavallini, M. C., Cellini, E., Di Bella, D., Erzegovesi, S., Foulon, C., Gabrovsek, M., Gorwood, P., Hebebrand, J., Hinney, A., Holliday, J., Hu, X., Karwautz, A., Kipman, A., … Estivill, X. (2004). Association of BDNF with anorexia, bulimia and age of onset of weight loss in six European populations. *Human Molecular Genetics*, *13*(12), 1205–1212. https://doi.org/10.1093/hmg/ddh137

Ridding, M. C., & Ziemann, U. (2010). Determinants of the induction of cortical plasticity by non-invasive brain stimulation in healthy subjects. *Journal of Physiology*, *588*(13), 2291–2304. https://doi.org/10.1113/jphysiol.2010.190314

Robinson, R. C., Radziejewski, C., Spraggon, G., Greenwald, J., Kostura, M. R., Burtnick, L. D., Stuart, D. I., Choe, S., & Jones, E. Y. (1999). The structures of the neurotrophin 4 homodimer and the brain-derived neurotrophic factor/neurotrophin 4 heterodimer reveal a common Trk-binding site. *Protein Science*, *8*(12), 2589–2597. http://www.pubmedcentral.nih.gov/articlerender.fcgi?artid=2144242&tool=pmcentrez&ren

dertype=abstract

Rosenfeld, R. D., Zeni, L., Haniu, M., Talvenheimo, J., Radka, S. F., Bennett, L., Miller, J. A., & Welcher, A. A. (1995). Purification and identification of brain-derived neurotrophic factor from human serum. *Protein Expression and Purification*, *6*(4), 465–471. https://doi.org/10.1006/prep.1995.1062

Schaefer, A., Kong, R., Gordon, E. M., Laumann, T. O., Zuo, X.-N., Holmes, A. J., Eickhoff, S. B., & Yeo, B. T. T. (2018). Local-Global Parcellation of the Human Cerebral Cortex from Intrinsic Functional Connectivity MRI. *Cerebral Cortex*, *28*(9), 3095. https://doi.org/10.1093/CERCOR/BHX179

Seiger, R., Ganger, S., Kranz, G. S., Hahn, A., & Lanzenberger, R. (2018). Cortical Thickness Estimations of FreeSurfer and the CAT12 Toolbox in Patients with Alzheimer's Disease and Healthy Controls. *Journal of Neuroimaging*, *28*(5), 515–523. https://doi.org/10.1111/JON.12521

Setton, R., Mwilambwe-Tshilobo, L., Girn, M., Lockrow, A. W., Baracchini, G., Hughes, C., Lowe, A. J., Cassidy, B. N., Li, J., Luh, W.-M., Bzdok, D., Leahy, R. M., Ge, T., Margulies, D. S., Misic, B., Bernhardt, B. C., Stevens, W. D., De Brigard, F., Kundu, P., … Spreng, R. N. (2022). Age differences in the functional architecture of the human brain. *Cerebral Cortex*. https://doi.org/10.1093/cercor/bhac056

Sheline, Y. I., & Raichle, M. E. (2013). Resting State Functional Connectivity in Preclinical Alzheimer's Disease. *Biological Psychiatry*, *74*, 340–347. https://doi.org/10.1016/j.biopsych.2012.11.028

Sidak, Z. (1967). Rectangular Confidence Regions for the Means of Multivariate Normal

Distributions. *Journal of the American Statistical Association*, *62*(318), 626. https://doi.org/10.2307/2283989

Sintini, I., Graff-Radford, J., Jones, D. T., Botha, H., Martin, P. R., Machulda, M. M., Schwarz, C. G., Senjem, M. L., Gunter, J. L., Jack, C. R., Lowe, V. J., Josephs, K. A., & Whitwell, J. L. (2021). Tau and Amyloid Relationships with Resting-state Functional Connectivity in Atypical Alzheimer's Disease. *Cerebral Cortex*, *31*(3), 1693–1706. https://doi.org/10.1093/CERCOR/BHAA319

Smit, D. J. A., Boomsma, D. I., Schnack, H. G., Hulshoff Pol, H. E., & de Geus, E. J. C. (2012). Individual Differences in EEG Spectral Power Reflect Genetic Variance in Gray and White Matter Volumes. *Twin Research and Human Genetics*, *15*(3), 384–392. https://doi.org/10.1017/thg.2012.6

Sohn, W. S., Yoo, K., Lee, Y. B., Seo, S. W., Na, D. L., & Jeong, Y. (2015). Influence of ROI selection on resting state functional connectivity: an individualized approach for resting state fMRI analysis. *Frontiers in Neuroscience*, *9*(JUL), 280. https://doi.org/10.3389/FNINS.2015.00280

Somers, M., Aukes, M. F., Ophoff, R. A., Boks, M. P., Fleer, W., de Visser, K. (C. . L., Kahn, R. S., & Sommer, I. E. (2015). On the relationship between degree of hand-preference and degree of language lateralization. *Brain and Language*, *144*, 10–15. https://doi.org/10.1016/j.bandl.2015.03.006

Sporns, O. (2011). *Networks of the brain.* MIT Press.

Spreng, R. N., Sepulcre, J., Turner, G. R., Stevens, W. D., & Schacter, D. L. (2013). Intrinsic architecture underlying the relations among the default, dorsal attention, and frontoparietal

control networks of the human brain. *Journal of Cognitive Neuroscience*, *25*(1), 74–86. https://doi.org/10.1162/jocn_a_00281

Spreng, R. N., Stevens, W. D., Chamberlain, J. P., Gilmore, A. W., & Schacter, D. L. (2010). Default network activity, coupled with the frontoparietal control network, supports goal-directed cognition. *NeuroImage*, *53*(1), 303–317. https://doi.org/10.1016/j.neuroimage.2010.06.016

Spreng, R. N., Stevens, W. D., Viviano, J. D., & Schacter, D. L. (2016). Attenuated anticorrelation between the default and dorsal attention networks with aging: Evidence from task and rest. *Neurobiology of Aging*, *45*, 149. https://doi.org/10.1016/J.NEUROBIOLAGING.2016.05.020

Stevens, W. D., & Spreng, R. N. (2014). Resting-state functional connectivity MRI reveals active processes central to cognition. *Wiley Interdisciplinary Reviews: Cognitive Science*, *5*(2), 233–245. https://doi.org/10.1002/wcs.1275

Suárez, L. E., Markello, R. D., Betzel, R. F., & Misic, B. (2020). Linking Structure and Function in Macroscale Brain Networks. *Trends in Cognitive Sciences*, *24*(4), 302–315. https://doi.org/10.1016/J.TICS.2020.01.008

Sutherland, M. T., McHugh, M. J., Pariyadath, V., & Stein, E. A. (2012). Resting state functional connectivity in addiction: Lessons learned and a road ahead. *NeuroImage*, *62*(4), 2281–2295. https://doi.org/10.1016/j.neuroimage.2012.01.117

Szeszko, P. R., Lipsky, R., Mentschel, C., Robinson, D., Gunduz-Bruce, H., Sevy, S., Ashtari, M., Napolitano, B., Bilder, R. M., Kane, J. M., Goldman, D., & Malhotra, A. K. (2005). Brain-derived neurotrophic factor Val66met polymorphism and volume of the hippocampal

formation. *Molecular Psychiatry*, *10*(7), 631–636. https://doi.org/10.1038/sj.mp.4001656

Szucs, D., & Ioannidis, J. P. (2020). Sample size evolution in neuroimaging research: An evaluation of highly-cited studies (1990–2012) and of latest practices (2017–2018) in high-impact journals. *NeuroImage*, *221*(October 2019), 117164. https://doi.org/10.1016/j.neuroimage.2020.117164

Thomason, M. E., Yoo, D. J., Glover, G. H., & Gotlib, I. H. (2009). BDNF genotype modulates resting functional connectivity in children. *Frontiers in Human Neuroscience*, *3*, 1–10. https://doi.org/10.3389/neuro.09.055.2009

Toro, R., Chupin, M., Garnero, L., Leonard, G., Perron, M., Pike, B., Pitiot, A., Richer, L., Veillette, S., Pausova, Z., & Paus, T. (2009). Brain volumes and Val66Met polymorphism of the BDNF gene: Local or global effects? *Brain Structure and Function*, *213*(6), 501–509. https://doi.org/10.1007/s00429-009-0203-y

Tost, H., Alam, T., Geramita, M., Rebsch, C., Kolachana, B., Dickinson, D., Verchinski, B. A., Lemaitre, H., Barnett, A. S., Trampush, J. W., Weinberger, D. R., & Marenco, S. (2013). Effects of the BDNF val 66 met polymorphism on white matter microstructure in healthy adults. *Neuropsychopharmacology*, *38*(3), 525–532. https://doi.org/10.1038/npp.2012.214

Van Essen, D. C., Smith, S. M., Barch, D. M., Behrens, T. E. J., Yacoub, E., & Ugurbil, K. (2013). The WU-Minn Human Connectome Project: An overview. *NeuroImage*, *80*, 62–79. https://doi.org/10.1016/j.neuroimage.2013.05.041

Walsh, V., Ellison, A., Battelli, L., & Cowey, A. (1998). Task–specific impairments and enhancements induced by magnetic stimulation of human visual area V5. *Proceedings of the Royal Society of London. Series B: Biological Sciences*, *265*(1395), 537–543.

https://doi.org/10.1098/rspb.1998.0328

Wang, C., Zhang, Y., Liu, B., Long, H., Yu, C., & Jiang, T. (2014). Dosage Effects of BDNF Val66Met Polymorphism on Cortical Surface Area and Functional Connectivity. *Journal of Neuroscience*, *34*(7), 2645–2651. https://doi.org/10.1523/JNEUROSCI.3501-13.2014

Wang, D., Buckner, R. L., Fox, M. D., Holt, D. J., Holmes, A. J., Stoecklein, S., Langs, G., Pan, R., Qian, T., Li, K., Baker, J. T., Stufflebeam, S. M., Wang, K., Wang, X., Hong, B., & Liu, H. (2015). Parcellating cortical functional networks in individuals. *Nature Neuroscience 2015 18:12*, *18*(12), 1853–1860. https://doi.org/10.1038/nn.4164

Wilcoxon, F. (1945). Individual Comparisons by Ranking Methods. *Bulletin*, *1*(6), 80–83. https://www.jstor.org/stable/3001968

Woodward, N. D., & Cascio, C. J. (2015). Resting-State Functional Connectivity in Psychiatric Disorders. *JAMA Psychiatry*, *72*(8), 743–744. https://doi.org/10.1001/JAMAPSYCHIATRY.2015.0484

Xing, J., Ginty, D. D., & Greenberg, M. E. (1996). Coupling of the RAS-MAPK pathway to gene activation by RSK2, a growth factor-regulated CREB kinase. *Science*, *273*(5277), 959–963. https://doi.org/10.1126/science.273.5277.959

Xu, B., Gottschalk, W., Chow, A., Wilson, R. I., Schnell, E., Zang, K., Wang, D., Nicoll, R. A., Lu, B., & Reichardt, L. F. (2000). The role of brain-derived neurotrophic factor receptors in the mature hippocampus: Modulation of long-term potentiation through a presynaptic mechanism involving trkB. *Journal of Neuroscience*, *20*(18), 6888–6897. https://doi.org/10.1523/jneurosci.20-18-06888.2000

Yan, T., Wang, L., Kuang, W., Xu, J., Li, S., Chen, J., & Yang, Y. (2014). Brain-derived neurotrophic factor Val66Met polymorphism association with antidepressant efficacy: A systematic review and meta-analysis. *Asia-Pacific Psychiatry*, *6*(3), 241–251. https://doi.org/10.1111/appy.12148

Yang, G., Li, D., Rao, Y., & Lu, F. (2020). The relationship between cortical thickness and language comprehension varies with sex in healthy young adults: A large sample analysis. *NeuroReport*, 184–188. https://doi.org/10.1097/WNR.0000000000001393

Yang, X., Liu, P., Sun, J., Wang, G., Zeng, F., Yuan, K., Liu, J., Dong, M., von Deneen, K. M., Qin, W., & Tian, J. (2012). Impact of Brain-Derived Neurotrophic Factor Val66Met Polymorphism on Cortical Thickness and Voxel-Based Morphometry in Healthy Chinese Young Adults. *PLoS ONE*, *7*(6). https://doi.org/10.1371/JOURNAL.PONE.0037777

Yeo, B. T., Krienen, F. M., Sepulcre, J., Sabuncu, M. R., Lashkari, D., Hollinshead, M., Roffman, J. L., Smoller, J. W., Zöllei, L., Polimeni, J. R., Fisch, B., Liu, H., & Buckner, R. L. (2011). The organization of the human cerebral cortex estimated by intrinsic functional connectivity. *Journal of Neurophysiology*, *106*(3), 1125–1165. https://doi.org/10.1152/jn.00338.2011

Appendix A

Number of participants excluded based on exclusion criteria for the Val/Val, Val/Met, and Met/Met groups.

Category	Val/Val	Val/Met	Met/Met	Total remaining
Positive drug test	21	4	0	367
Breathalyzer over .05% blood alcohol content	1	0	0	366
Father history of psychiatric disorder	13	12	0	341
Mother history of psychiatric disorder	11	11	0	319
Handedness	21	14	0	284
Quality control flag for motion	3	0	0	281

Table A. From a total of 1029 participants with both GPIP parcellations and genetic data available, the participants were randomly selected such that only one member of each family group was selected (n = 392). The additional exclusion criteria listed here were included due to potential influence on RSFC, resulting in a total of n = 281 participants in the functional analysis. Drug tests included THC, cocaine, opiates, amphetamines, methamphetamines, and oxycontin. Father and mother history of psychiatric disorder were reported by the participant. Handedness was measured using the Edinburgh Handedness Inventory (Oldfield, 1971). Participants flagged for motion had one or more rfMRI scans with a significant coil- or movement-related artifact.